

Engine Modeling of an Internal Combustion Engine
With Twin Independent Cam Phasing

THESIS

Presented in Partial Fulfillment of the Requirements for
Graduation with Distinction at
The Ohio State University

By
Jason Meyer

* * * * *

The Ohio State University
2007

Defense Committee:
Professor Yann Guezennec, Advisor
Professor James Schmiedeler

Approved by

Adviser
Undergraduate Program in Mechanical
Engineering

Copyright

Jason Meyer

2007

Table of Contents

Table of Contents	1
Table of Figures	3
Acknowledgements	5
Abstract	6
Chapter 1: Introduction	7
Chapter 2: Literature Review	9
2.1. Variable Valve Actuation Introduction	9
2.2 Types of Variable Valve Actuation	12
2.2.1 Discretely-Stage Cam Systems	12
2.2.2 Continuously Variable Cam Systems	13
2.2.3 Cam Phasing	15
2.2.4 Cam Independent Variable Valve Actuation	18
2.3 Load Control	18
2.3.1 Optimum Low Load VVA Techniques	19
2.3.2 Optimum High and Full Load VVA Techniques	20
2.4 Internal Exhaust Gas Recirculation	20
2.4.1 Idle and Low Speed EGR Requirements	21
2.4.2 Moderate and Full Load EGR Requirements	22
2.4.3 Drawbacks of Internal EGR	23
2.5 Variable Compression Ratios	23
2.6 Cost Considerations	24
2.7 Conclusions on Variable Valve Actuation	25
Chapter 3: Experimental Methodology	26
3.1. Project Goals	26
3.2. Mapping an Engine	26
3.3 Engine Setup	28
3.4 Experimental Procedure	30
3.5 Engine Simulations	32
3.6 How GT-Power Generates a Solution	33
3.7 GT-Power Model Creation	34
3.7.1 Ambient Air Volume	36
3.7.2 Lumped Throttle	36
3.7.3 Piping for the Intake and Exhaust Systems	37
3.7.5 Intake and Exhaust Cam Profiles	38
3.7.6 Engine Block	38
3.8 Engine Model Validation	39
Chapter 4: Data Analysis	40
4.1 Combustion Modeling	40
4.3 Heat Release Calculations	43
4.4 Mass Fraction Burned Curves	44
4.5 Modeling Difficulties of Mass Fraction Burn Curves	46
4.6 Variations in Mass Fraction Burned Approximation's Constants	49
4.7 Coefficient Prediction Using a Step-wise Multivariable Regression	51
4.8 Results from Initial Regression	52

4.9 Grouping the Data into Regions	54
4.10 Predictive Ability of Regression Equations after Grouping	57
Chapter 5: Results.....	59
5.1 GT-Power’s Crank Angle Resolved Capabilities.....	59
5.2 GT-Power Cycle Average Capabilities	70
Chapter 6: Conclusions	89
Chapter 7: Future Research	90

Table of Figures

Figure 1: Efficiency Map of a Typical SI Engine (Guezennec, 2003)	10
Figure 2: Torque Curve Comparison	11
Figure 3: Typical Discretely Staged Cam Setup (Hatano, 1993).....	13
Figure 4: Continuously Variable Roller Follower Arm (Pierik and Burkhard, 2000).....	14
Figure 5: Cam Profiles Possible with Continuously Variable VVA (Pierik and Burkhard, 2000)	14
Figure 6: Cam Phasing Technology (Moriya, 1996)	15
Figure 7: Valve Lift for an Engine with Cam Phasing (From Moriya, 1996)	16
Figure 8: Pressure-Volume Effect of Cam Phasing (Tabaczynski, 2002)	17
Figure 9: Effects of EIVC and LIVO on Valve Lift (Centro Ricerche Fiat, 2002)	17
Figure 10: Intake and Exhaust Timing Strategies depending on Loading (Kramer and Philips, 2002)	19
Figure 11: Optimum Timing and Lift Chart (Heywood, 1988)	20
Figure 12: Methods of EGR Control (FEV Motortechnik, 2002)	22
Figure 13: Picture of the Engine Experimental Setup	29
Figure 14: Distribution of Operating Points	31
Figure 15: Illustration of Component Discretization (GT-Power Manual, 2004).....	33
Figure 16: Example of a GT-Power Model	35
Figure 17: Part Definition Window	36
Figure 18: Final GT-Power Model	39
Figure 19: Representative Wiebe Curve	41
Figure 20: Variation in Mass Fraction Burned Curves	45
Figure 21: Representative Mass Fraction Burned Curve Comparison	45
Figure 22: In-cylinder Pressure Trace of Two Mode Combustion	46
Figure 23: Experimental Data fit to a Wiebe Approximation.....	47
Figure 24: Mass Fraction Burned Data and Approximation Comparison	48
Figure 25: Variation in Mass Fraction Burned Approximation Coefficients	49
Figure 26: Comparison between Measured Mass Fraction Burned Curve and Approximation using the Average Coefficients	50
Figure 27: Comparison between Experimental and Approximated Values of Coefficient x	53
Figure 28: Boundaries for each Data's Region.....	55
Figure 29: Comparison of Experimental and Approximated Values of AI	56
Figure 30: Comparison between Predicted and Experimental Mass Fraction Burned Curves	57
Figure 31: Error Statistics of Mass Fraction Burned Prediction by Region	58
Figure 32: Intake Valve Lift and Velocity (1500 rpm, 0.3 bar).....	60
Figure 33: Exhaust Valve Lift and Velocity (1500 rpm, 0.3 bar).....	60
Figure 34: Wave Dynamics of the Intake System (1500 rpm, 0.3 bar)	61
Figure 35: Wall Temperature of the Intake System (1500 rpm, 0.3 bar).....	62
Figure 36: Charge Temperature of the Intake System (1500 rpm, 0.3 bar).....	63
Figure 37: Mass Flow of Air through the Throttle (1500 rpm, 0.3 bar)	64

Figure 38: Pressure Drop across the Throttle (1500 rpm, 0.3 bar)	65
Figure 39: Manifold Air Pressure (1500 rpm, 0.3 bar)	65
Figure 40: Mass Flow of Injected Fuel (1500 rpm, 0.3 bar)	67
Figure 41: In-cylinder Pressure (1500 rpm, 0.3 bar)	67
Figure 42: Pressure-Volume Diagram (1500 rpm, 0.3 bar)	68
Figure 43: Normalized Cumulative Burn Rate (1500 rpm, 0.3 bar)	69
Figure 44: Normalized Apparent Heat Release Rate (1500 rpm, 0.3 bar)	69
Figure 45: Overall Output Torque (1500 rpm, 0.3 bar)	70
Figure 46: Operating Points Encountered during a FTP Cycle (2000 rpm, 0.49 bar)	71
Figure 47: Effect of Cam Timing on IMEP (2000 rpm, 0.49 bar)	72
Figure 48: Effect of Cam Timing on Trapped Air Mass (2000 rpm, 0.49 bar)	74
Figure 49: Effect of Cam Timing on Indicated Fuel Conversion Efficiency (2000 rpm, 0.49 bar)	75
Figure 50: Effect of Cam Timing on Trapped Residual Gases (2000 rpm, 0.49 bar)	77
Figure 51: Effect of Cam Timing on Residual Gas Fraction (2000 rpm, 0.49 bar)	78
Figure 52: Effect of Cam Timing on Air Charge Temperature (2000 rpm, 0.49 bar)	80
Figure 53: Effect of Cam Timing on Volumetric Efficiency (2000 rpm, 0.49 bar)	81
Figure 54: Effect of Cam Timing on Manifold Volumetric Efficiency (2000 rpm, 0.49 bar)	83
Figure 55: Effect of Cam Timing on the Combustion Duration (2000 rpm, 0.49 bar)	84
Figure 56: Effect of Cam Timing on the Start of Combustion (2000 rpm, 0.49 bar)	86
Figure 57: In-cylinder Pressure Evolution (2000 rpm, 0.49 bar)	87
Figure 58: Variations in Mass Fraction Burned Curved (2000 rpm, 0.49 bar)	88

Acknowledgements

A number of people and institutions have been a great inspiration and have helped me. General Motors provided a great deal of technical support especially Dr. Ken Dudek and Layne Wiggins. In addition, I would thank my advisor Dr. Yann Guezennec who has guided me through my research. Even with a hectic schedule, he was able to provide feedback and insight. Dr. Shawn Midlam-Mohler is another person who has always been available to answer questions. Two graduate students have also assisted me in my research. I would like to thank Ben Montello and Adam Vosz. Finally, I would also like to thank The Ohio State University, the Mechanical Engineering department and the Center for Automotive Research.

Abstract

In the modern world, one of the largest concerns is the ever depleting supply of oil. The automotive industry is especially impacted. In recent years the price of gasoline has fluctuated substantially and the price of crude oil has reached record highs. The high price of gasoline coupled with the uncertainty of its availability and future price have put a high priority on fuel economy of an engine. In addition the emissions released from internal combustion (IC) engines are polluting the atmosphere. Many studies have linked the greenhouse gases produced by an automobile engine to the partial destruction of our atmosphere and to global warming. As a result the US government is passing stricter and stricter emissions regulations.

These major issues are putting pressure on automakers to develop new technologies to increase the fuel economy and decrease the emissions while maintaining or improving the engine's performance. Several new technologies have resulted. All of these technologies accomplish these goals by increasing the efficiency of an engine. As a whole these technologies are called variable valve actuation. These technologies achieve a higher efficiency by reducing the constants of the engine. However, the added variability increases the time to calibrate an engine. To address this, more testing is being performed using engine simulations instead of physical testing. This thesis focuses on how to create an engine model and how engine simulation can be used to optimize such an engine. In addition the benefits of a particular variable valve actuation technology, cam phasing, will be explored.

Chapter 1: Introduction

The design of an internal combustion (IC) engine is a complex compromise between performance, fuel economy and emissions. These three factors are interrelated and they cannot be simultaneously optimized. Furthermore once the physical parameters such as displacement, cam profile and compression ratio are determined, a conventional engine has nearly fixed performance, fuel economy and emissions properties. By making an engine more efficient, one or more of these factors could be increased without significantly compromising the others.

Thermodynamics shows that the higher an engine's compression ratio, the higher its efficiency. However, the in-cylinder pressures and temperatures which result from higher compression ratios place an upper bound on an engine's compression ratio. The cause of this limiting is largely engine knock or auto-ignition. When an engine starts knocking, the progressive normal combustion is replaced by very fast detonation waves in the combustion chamber, and the engine can be severely damaged. Another method of increasing the efficiency of an engine is reducing the mechanical losses associated with throttling. When an engine is throttling, a plate obstructs the air intake flow and causes a pressure drop across the plate. Throttling reduces the amount of air induced into the engine, but it introduces flow losses which reduce an engine's efficiency.

A conventional engine has static, mechanically-actuated valves and a compression ratio that is fixed once the components of the engine are chosen. A recently developed technology called variable valve actuation (VVA) enables added control of valve timing, lift and/or duration. With this additional freedom, the efficiency of an engine can be

greatly increased. Not only can the compression ratio be increased with the addition of VVA, but also the necessity of throttling can be reduced.

Although cam phasing has numerous benefits, it also has significant drawbacks. The largest drawback is a substantial increase in the amount of testing required to create an optimized engine map. By using engine modeling, the amount of testing required is reduced because most of the testing is done virtually through a simulation. The creating of an engine model requires a broad range of experimental data. To make an accurate model, the data must span the entire range of operating conditions. However, only a relatively small amount of data is needed. This thesis focuses on how to create an engine model and how to use the model to optimize engine development. In this study the abilities of GT-Power, an engine simulation program, will specifically be explored. Both the cycle resolved and cycle averaged data will be presented. The simulations will show the effect of intake and exhaust cam phasing on the trapped air mass, the trapped residual gases, intake air temperature, indicated mean effective pressure and combustion stability.

Chapter 2: Literature Review

2.1. Variable Valve Actuation Introduction

Conventional engines are designed with fixed mechanically-actuated valves. The position of the crankshaft and the profile of the camshaft determine the valve events (*i.e.*, the timing of the opening and closing of the intake and exhaust valves). Since conventional engines have valve motion that is mechanically dependent on the crankshaft position, the valve motion is constant for all operating conditions. The ideal scheduling of the valve events, however, differs greatly between different operating conditions. This represents a significant compromise in an engine's design.

In standard IC engines, the compression ratio (set by the engine's mechanical design) is also fixed for all engine conditions. The compression rate is thus limited by the engine condition with the lowest knock limit. Engine knock is caused by spontaneous combustion of fuel without a spark (auto-ignition). For spontaneous combustion to occur, the temperature and pressure must be sufficiently high. Therefore the limiting condition occurs at wide open throttle (WOT) and engine speeds close to redline. Likewise, lower engine speeds and throttled conditions (the most common operating conditions when driving a vehicle) have much less tendency to knock and can withstand higher compression ratios (hence the potential for higher efficiency).

The most common operating conditions for IC engines are low engine speeds and moderately throttled air flow. Unfortunately, the optimum conditions for the average IC engine are at WOT and low to moderate engine speeds. Throttling the intake air creates fluid friction and pumping losses. High engine speeds create greater mechanical friction thus reducing the efficiency. Figure 1 is an efficiency map of an engine with the most

common operating region indicated. If the typical operating efficiency of the engine was improved, then the fuel economy would greatly increase.

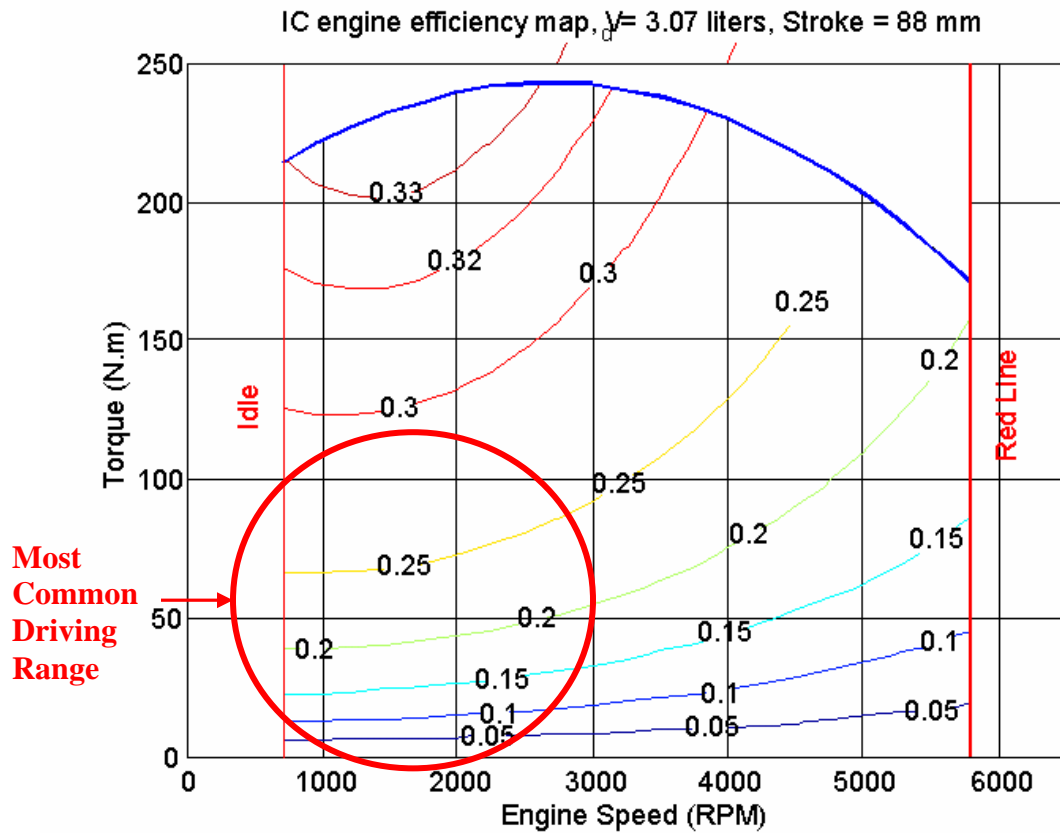


Figure 1: Efficiency Map of a Typical SI Engine (Guezennec, 2003)

The most common use of VVA is load control. A normal engine uses throttling to control the load of the engine. When an engine is throttled, the flow separation created from a throttle body creates fluid losses and the volumetric efficiency decreases. A major goal of a VVA engine is to control the amount of air inducted into the engine without a physical restriction in the flow field.

The torque curve of a conventional engine has a very distinct peak that generally occurs in the middle of the engine speed range. The torque produced at low engine speeds is much less because the incoming mixture of fuel and air is at a comparatively

low velocity. To increase the torque at low engine speeds, the intake valve should close right after the piston passes the bottom dead center (BDC) between the intake and compression strokes. This will effectively generate a maximum compression ratio for low engine speeds. Increasing the compression ratio at low engine speeds essentially pushes the engine closer to a loaded condition. Conversely at high speeds, the velocity of the intake mixture is large. Thus the optimum condition is where the intake valve stays open longer. The torque curve comparison between conventional and VVA engines is shown in Figure 2.

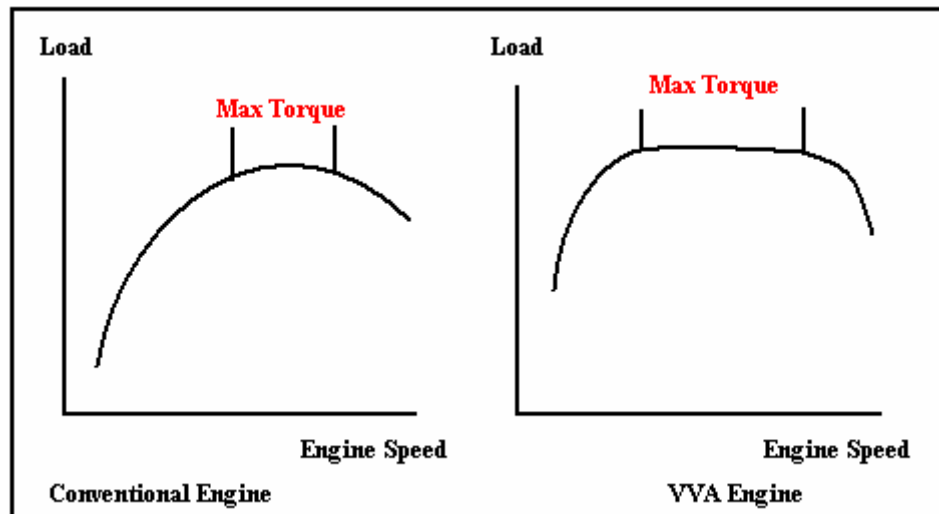


Figure 2: Torque Curve Comparison

Another major use of VVA is internal exhaust gas recirculation (Internal EGR or IEGR). The residual burn fraction is important for all engine conditions. At low engine speeds the percent of EGR should be small, because combustion is already unstable. Moreover, adding combustion products to the intake charge only reduces the combustibility. At higher speeds EGR can actually increase the efficiency and help produce more power. EGR is also important in limiting the emissions of an engine and reducing engine knock.

2.2 Types of Variable Valve Actuation

Engines with VVA can be categorized by their method of actuation. The three categories are electrohydraulic, electromechanical and cam-based actuators. The first two categories are mainly investigated today as potential future technologies, but they are not technologically ready for use in a production engine. On the other hand, cam-based actuation is quickly becoming the standard on many production engines. Thereby maximizing their potential benefits has been the topic of significant research and development. Cam-based actuators can be further categorized into variable valve timing (VVT) systems, discretely-staged cam-profile switching systems, and continuously-variable cam-profile systems. Discretely-staged cam-profile switching systems generally have two or possibly three different cam profiles that can be switched between. Continuously-variable cam-profile systems have a profile with a constant shape, but the amplitude can be increased or decreased within a range of values. Variable valve timing (VVT) is able to change the valve timings but not the valve lift profiles and durations. The camshafts can only be advanced or retarded in regard to its neutral position on the crankshaft. VVT can be controlled by a hydraulic actuator called a cam phaser. Engines can have a single cam phaser (intake cam only) or two cam phasers (both intake and exhaust cams).

2.2.1 Discretely-Stage Cam Systems

A dual cam engine has one cam to control the intake and one cam to control the exhaust valve events. The profile of the cam determines the timing, the lift and the duration of the valve opening. Conventionally, these cam profiles control the valve event throughout the entire engine operation range. The camshaft would therefore have one

lobe per cylinder. One major branch of VVA, called discretely staged cam VVA, replaces this standard camshaft with a camshaft with two lobes per cylinder. The lobes have drastically different profiles. Figure 3 shows a picture of a typical discretely staged cam VVA camshaft and rocker arm. The lift profile of each cam lobe is also displayed. One profile is very shallow and is used for low engine loads. The second profile is used when high engine performance is necessary. This profile is very tall to induct as much air as possible. Another very similar solution is to have two separate roller follower arms reading a common profile, instead of two separate cam profiles. In this solution the high speed roller arm is much closer to the camshaft than the low speed arm.

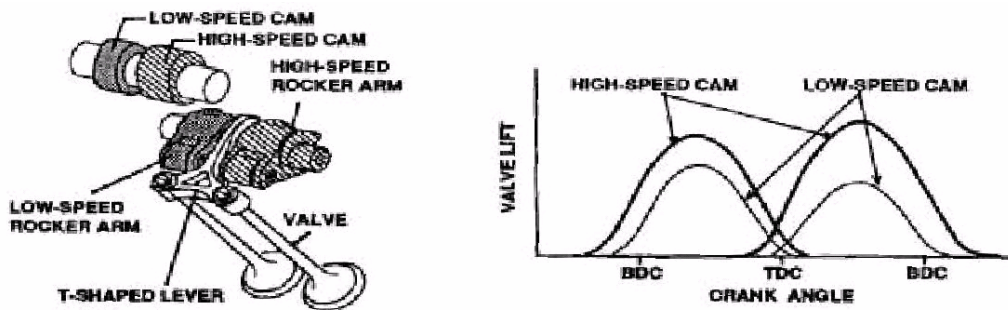


Figure 3: Typical Discretely Staged Cam Setup (Hatano, 1993)

2.2.2 Continuously Variable Cam Systems

A step further in VVA development is a continuously variable cam profile. This is accomplished with a movable roller follower arm. A normal roller follower does not move, so the distance away from the camshaft is fixed. An engine with a movable roller follower arm is able to control the distance to the camshaft and thus the amount of valve lift. An illustration of a continuously variable roller follower arm is presented in Figure 4. By increasing the distance from the camshaft, the minimum height on the cam that will open the valves is increased. This technology therefore can have an infinite number

of possible valve events. Figure 5 shows the some of the possible valve lift profiles. As seen by the graph, the profiles have similar shapes but have varying amplitudes.

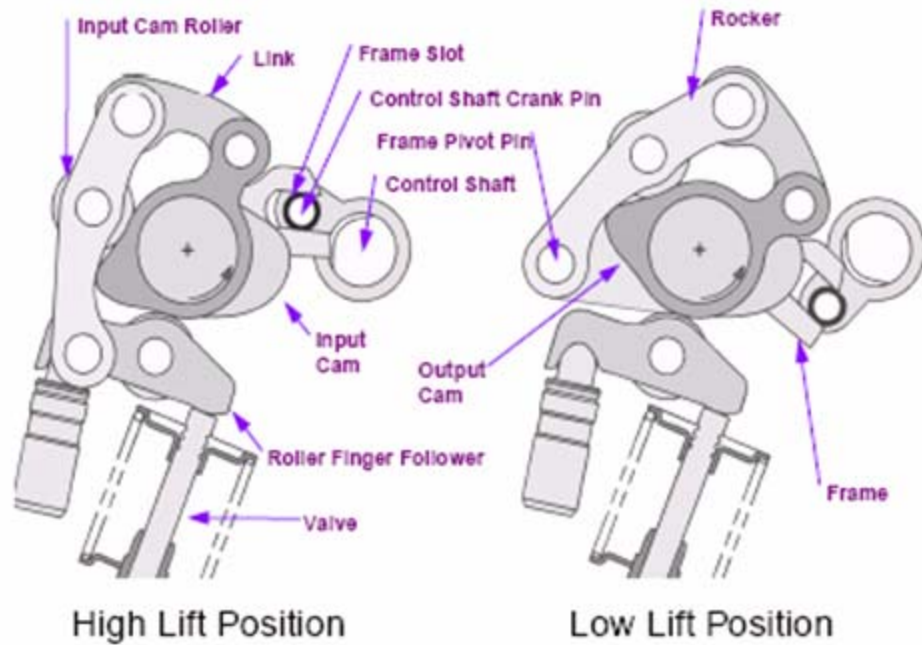


Figure 4: Continuously Variable Roller Follower Arm (Pierik and Burkhard, 2000)

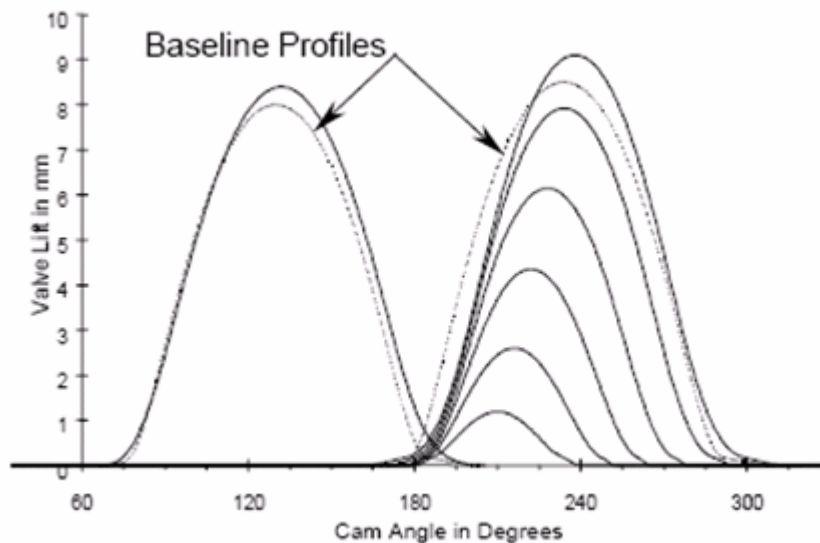


Figure 5: Cam Profiles Possible with Continuously Variable VVA (Pierik and Burkhard, 2000)

2.2.3 Cam Phasing

Another continuously variable VVA technology, cam phasing, focuses on cam timing instead of cam profiles. Cam phasing is a cam based technology that controls the phase of the camshaft in relation to the crankshaft. An engine with an intake cam phaser is shown in Figure 6. The typical cam phasing engine has a phasing range of about 40 to 60 degrees. The valve lift of an engine with cam phasing is presented in Figure 7. Although the effect of cam phasing may seem minor, it is actually one of the most robust technologies. One of the major goals of VVA is the control of the air flowing into the cylinders. The two previous technologies achieved this by controlling the valve lift. With cam phasing the amount of air ingested into the combustion chamber is controlled by either early intake valve opening (EIVO) or late intake valve opening (LIVO).

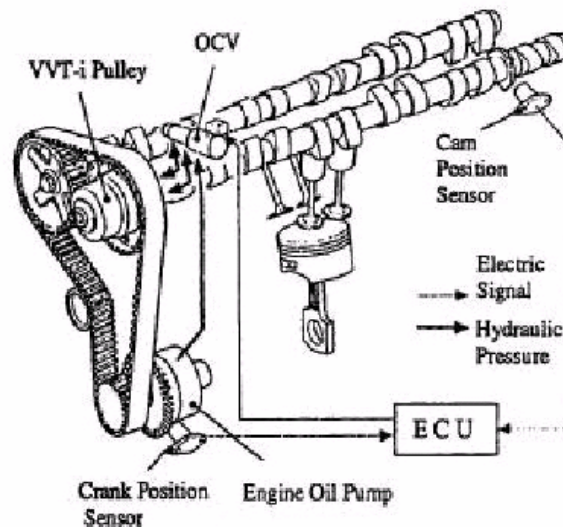


Figure 6: Cam Phasing Technology (Moriya, 1996)

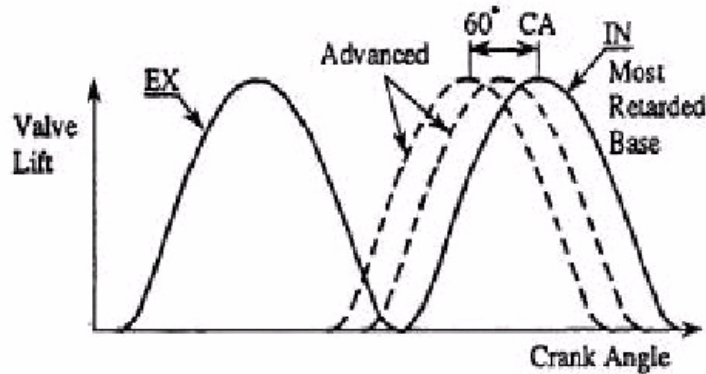


Figure 7: Valve Lift for an Engine with Cam Phasing (From Moriya, 1996)

With early intake valve opening (EIVO) the intake valves are opened well before top dead center (TDC) of the crankshaft. The intake valves then close before the crankshaft reaches bottom dead center (BDC). The displaced volume is therefore much less than normal. Late intake valve closing (LIVC) does nearly the exact opposite. For LIVC the intake valves are opened at about TDC and then remain open past BDC. At high engine speeds the intake charge has a large momentum and will continue to fill the combustion chamber even after BDC. LIVC increases the volumetric efficiency at high speeds.

Cam phasing of the exhaust cam can also allow for easier control of exhaust gas recirculation. The timing of the intake valve opening and closing can alter the effective compression ratio while also changing the expansion ratio. Figure 8 illustrates the difference in pressure-volume (p-V) diagrams between throttling, EIVC and LIVC. Figure 8 also shows the pumping work (the lower loop in the p-V diagram) for EIVC and LIVC is much less than throttling, hence further contributing to efficiency gains. The valve lift profiles for late intake valve opening and early intake valve closing are shown in Figure 9. LIVC has the same effect as the other VVA technologies, namely the

profiles are the same shape as the baseline but with lower amplitudes. EIVC, however, has an effect unique to cam phasing. The effect is a high amplitude profile with a short duration that peaks quickly after TDC.

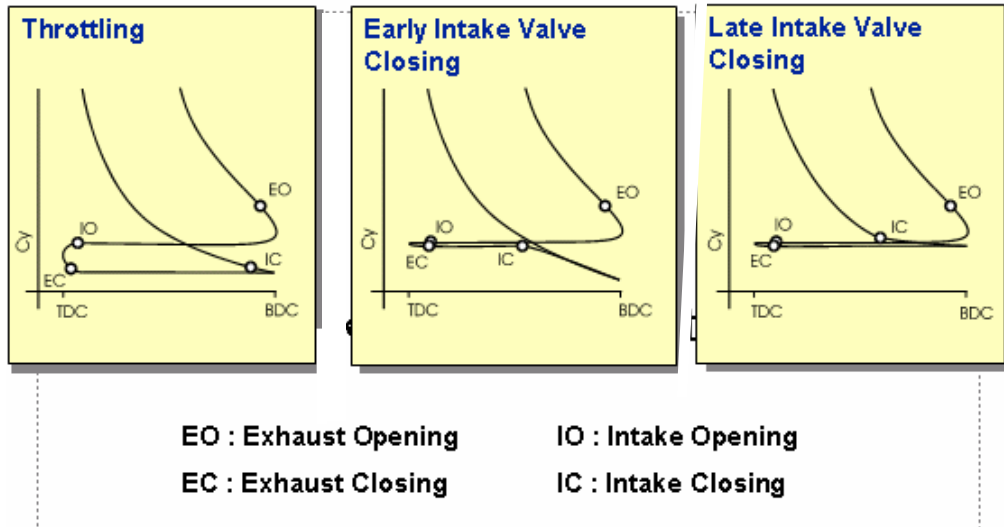


Figure 8: Pressure-Volume Effect of Cam Phasing (Tabaczynski, 2002)

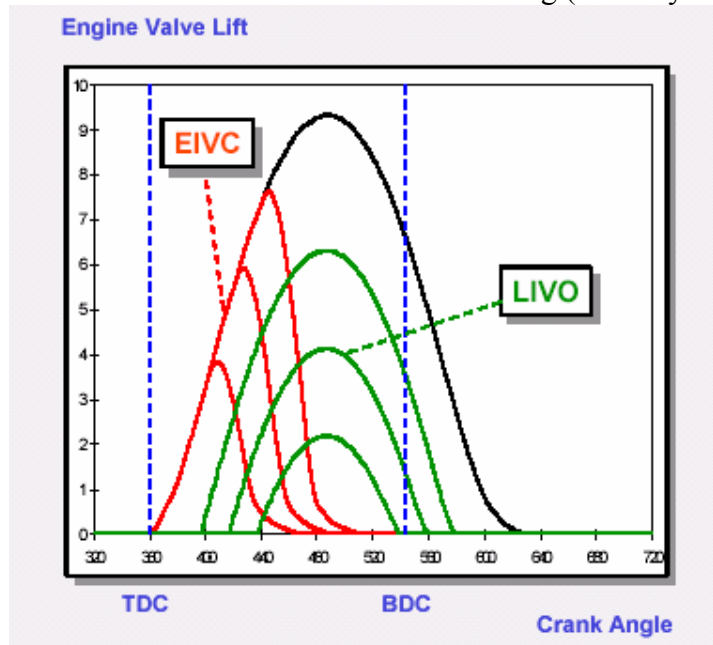


Figure 9: Effects of EIVC and LIVO on Valve Lift (Centro Ricerche Fiat, 2002)

2.2.4 Cam Independent Variable Valve Actuation

Another VVA technology removes the camshaft from the engine completely. Instead of having the camshaft control the valve events, they are controlled completely independently by either an electromechanical, hydroelectric or electromagnetic actuator. The valve timing, lift and duration can be controlled without limitation. Cylinder deactivation would also be possible. Without a need for camshafts, the engine's overall size could be reduced. This technology sounds promising, but it is still very experimental. Because the engine speeds are so high, the valves have very little time to respond to force inputs. The valve profiles would look more like a square wave instead of a gradual increase. This would likely create a great deal of noise. Another consideration is reliability and durability. Although it is not perfected yet, independent control of the valves theoretically has the most potential.

2.3 Load Control

As previously stated, load control is one the most significant effects of VVA. Using VVA to control the engine load significantly reduces the amount of pumping losses. The overall strategy for cam phasing is shown in Figure 10.

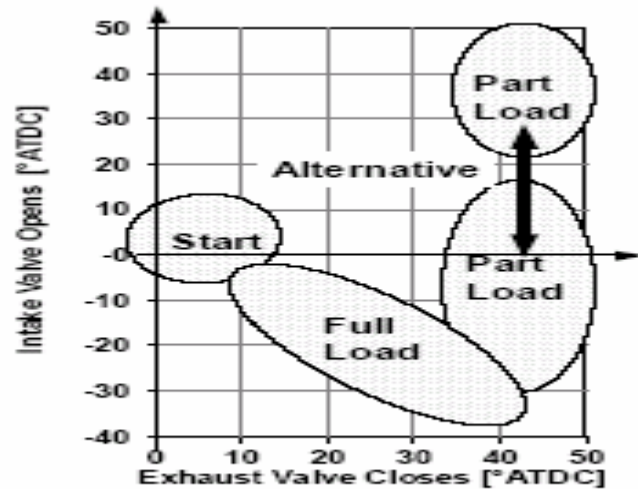


Figure 10: Intake and Exhaust Timing Strategies depending on Loading (Kramer and Philips, 2002)

2.3.1 Optimum Low Load VVA Techniques

Idle and part load conditions do not require a great deal of intake charge. Ideally this small amount of air would be inducted with minimal or without any throttling. Throttling the intake reduces the pressure in the intake system. This decreased pressure increases the area of the pumping loop and reduces the net power. The optimum low speed cam for discretely staged VVA is a low height and a moderate duration profile.

For cam phasing either LIVO or EIVC should be used. LIVO is more effective for cold start, and EIVC is more effective for warmed up engines (Sellnau, 2003). A study on a 1.6 liter 4-cylinder engine with twin cam phasing was done by Ulrich Kramer and Patrick Philips. They found that at 2000 rpm and 2 bar BMEP the fuel economy was increased by 7.5 percent by retarding both the intake and exhaust cams. LIVO increases the volumetric efficiency at low speeds by closing the intake valve right around BDC. EIVC reduces the amount of air inducted and eliminates the need for throttling.

2.3.2 Optimum High and Full Load VVA Techniques

At full load the efficient induction of air is the most important factor. Therefore, the intake cam should have a very steep and long profile. The profile should be as aggressive as possible within the knock limit. The valve overlap should be moderate to high to increase the residual gas fraction. The intake valves should be closed well after BDC to increase the volumetric efficiency. Figure 11 shows a graph of volumetric efficiency versus engine speed for three different valve timings. It also shows the volumetric efficiency versus valve lift. As the valve lift is increased, the volumetric efficiency increases. The maximum efficiency occurs when the valve lift creates an opening area equal to the port area.

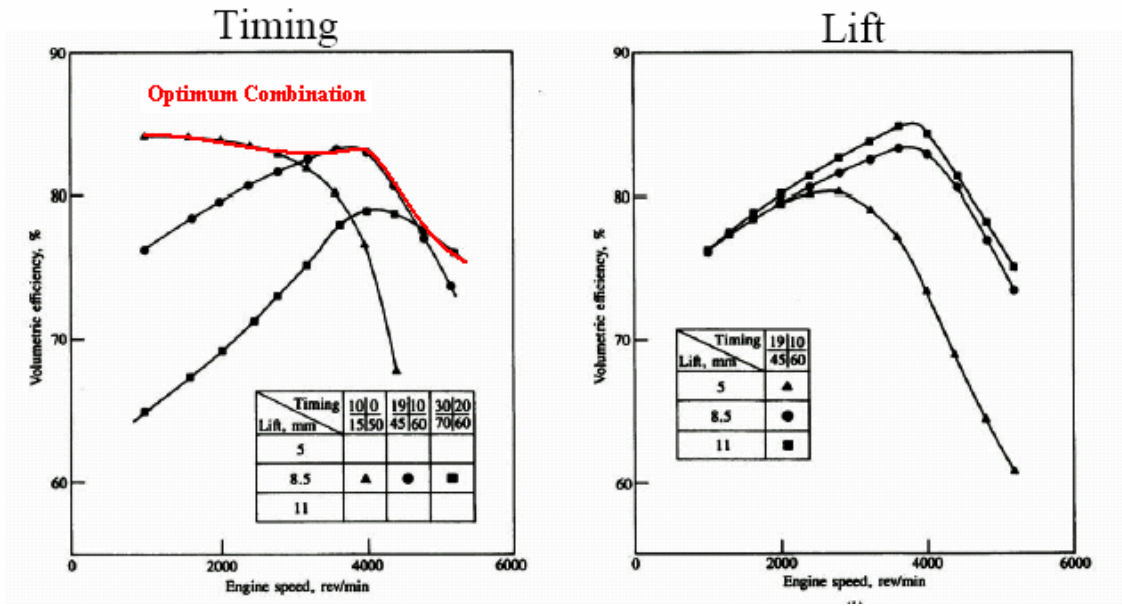


Figure 11: Optimum Timing and Lift Chart (Heywood, 1988)

2.4 Internal Exhaust Gas Recirculation

The thermodynamic efficiency is directly related to the peak temperature of combustion. Although it seems logical to increase the temperature of combustion, most

of the time the temperature of combustion is actively sought to be reduced. Too high of a combustion temperature has several effects. The first effect is emissions production, specifically NO_x. The concentration of NO_x produced by an engine is a strong function of temperature. Above about 2000 degrees Kelvin the NO_x formation increases dramatically. An increase in temperature from 2000 to 2500 degrees Kelvin increases the NO_x reaction rate by 10³ times.

Even if emissions were not a consideration, the thermal stresses on the engine create an upper bound for temperature. Another limiting factor is engine knock. As the temperature increases, the chance for engine knock also increases. The combination of higher cylinder wall temperatures and higher gas temperatures causes the air-fuel mixture to ignite before the spark plug can ignite the fuel.

2.4.1 Idle and Low Speed EGR Requirements

At idle speed and especially at cold start, EGR actually inhibits normal combustion. To ensure combustion during cold start, the ECU increases the fuel by a large amount. The addition of a non-reactive gas to the combustion mixture would be counterproductive. The optimum amount of EGR at idle is normally very small or zero. An engine can never have zero percent residual gas. From the physical geometry of the cylinder, the engine has some residual gases present. Since cylinders have some clearance volume, not all of the exhaust gases are expelled. To ensure the residual gas fraction is very small, the valve overlap is normally zero or negative (there is time between exhaust closing and intake opening). Figure 12 shows the major methods of controlling EGR. The top diagram of Figure 12 corresponds to negative valve overlap.

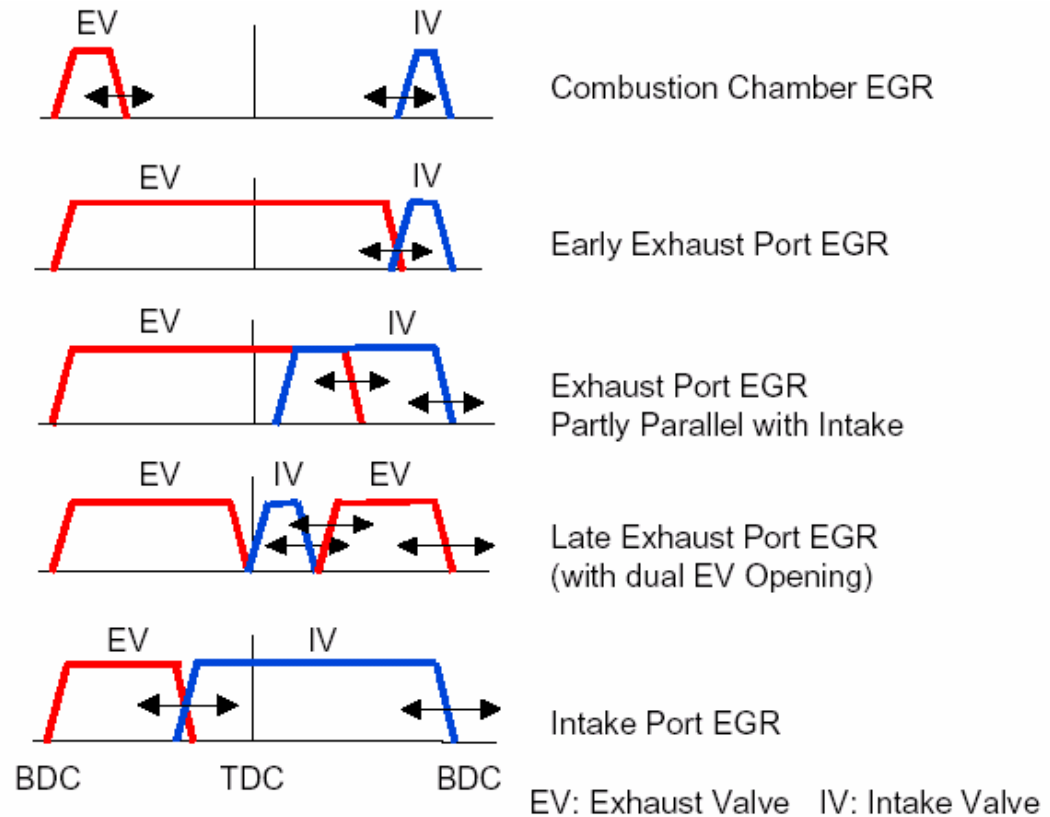


Figure 12: Methods of EGR Control (FEV Motortechnik, 2002)

2.4.2 Moderate and Full Load EGR Requirements

For higher speeds, EGR can be used in a variety of ways. The first method is load control. Since EGR will not combust, increasing EGR decreases the effective amount of air in the cylinder without throttling. This will reduce the pumping losses at part load conditions. The addition of EGR also reduces the amount of NO_x and hydrocarbon emissions produced. Several studies have found that increasing the EGR reduced the NO_x emission by up to 50 percent. Load control with EGR alone has only a limited effect, because the limit of EGR for normal combustion is low. Usually 20 percent EGR is the maximum amount that can be added. If too much EGR is added, then the combustion process is slowed down and combustion stability is reduced. Too much EGR

will also increase the hydrocarbon emissions. At wide open throttle EGR can be used as a knock reducer. The lower temperature achieved with the addition of EGR also reduces the likelihood of auto-ignition. This can allow the engine to operate at higher engine speeds and higher compression ratios. Valve overlap is used to increase the internal EGR of an engine. Depending on the operating condition, either the intake cam is advanced or the exhaust cam is retarded.

2.4.3 Drawbacks of Internal EGR

One of the major goals of EGR is to reduce the temperature of combustion. The addition of a noncombustible gas to the intake charge reduces the final combustion temperature. The intake temperature, however, is increased with the addition of EGR. External EGR is able to lower the temperature of the recirculated exhaust because some heat is transferred to EGR piping. Internal EGR is only able to transfer heat to the intake charge. This increase in temperature compared to standard EGR could have a variety of effects on the engine. One result could be an increased need for engine cooling.

2.5 Variable Compression Ratios

With cam phasing and continuously variable engines it is possible to have different effective compression ratios for different areas of engine operating conditions. By inducting different volumes of intake charge, the effective compression ratio would change. Every range could be set to have the highest compression ratio within its knock limit. The physical geometry of the engine could be increased to 12 or 13. At high speeds when engine knock is most probable, the displacement volume could be reduced. Since the clearance volume would remain constant, the compression ratio would

decrease. At high speeds, the power and efficiency would be comparable to an engine with a lower compression ratio. At low speeds, however, the efficiency would be higher.

As the compression ratio increases, the pressure at the end of compression also increases. This leads to higher pressure during and after combustion. The efficiency of combustion and the torque output is directly related to the pressure of combustion. Although a higher compression ratio means more torque and a higher efficiency, the increased pressure and temperature also contribute to a faster combustion speed and higher heat transfer. The increased combustion temperatures at low speeds can also lead to increased production of emissions and higher pollutant formation, particularly NO_x (nitric oxides). HOWEVER, the after-treatment catalyst can nearly eliminate this adverse effect.

2.6 Cost Considerations

Variable valve timing engines have many benefits, but they also cost more than standard engines. Not only is the hardware more expensive, but also a significantly more complex engine management code must be designed. In addition VVA engines require much more time to design. The addition of VVA variables increases the testing time needed to optimize an engine and increases the complexity of engine simulation software. For some applications the increase in cost of producing a VVA could overshadow the benefits of the technology. Most applications can benefit from VVA though.

Although VVA has an increased cost compared to their non-VVA counterparts, VVA engines are often a solution to increasing horsepower without increasing the number of cylinders or displacement. For example a four cylinder VVA engine could be a replacement for a standard V-6. The cost of adding VVA to a four cylinder engine is

often comparable to the increased cost of a V-6. A four cylinder VVA engine has many benefits over a standard V-6. A smaller four cylinder engine would not only have better fuel economy, but also would weigh less.

2.7 Conclusions on Variable Valve Actuation

In recent years the demand for engines with better performance has increased. In addition higher gas prices have increased the importance of fuel economy. Likewise, fears of global warming have resulted in stricter emissions standards. Variable valve actuation is a very cost effective and a reliable solution to all of these problems. VVA technologies can control internal EGR to reduce NO_x production, prevent engine knock and provide higher efficiency. In addition VVA technologies allow for optimization of volumetric efficiency over multiple engine conditions. The valve lift and duration can also be optimized for several different engine ranges to increase fuel economy and performance. Some forms of VVA can completely eliminate throttling to reduce pumping losses.

Chapter 3: Experimental Methodology

3.1. Project Goals

To try to reduce the time it takes to map out an engine with cam phasing, the combustion properties of an engine with cam phasing were studied. The initial goal was to take a small representative set of data and create an accurate engine model. This model would then be inputted into GT-Power and validated with a set of independently collected data. With this combustion model, the complete engine map would be created. The dependence of spark or fuel delivery on valve timing was assumed to be negligible, and the spark timing and fuel delivery were already mapped for this engine. Therefore, the existing spark timing and fuel delivery maps were used. With that simplification each data point is defined by only four variables. These variables are intake cam position, exhaust cam position, engine speed and manifold air pressure (load).

After the model is generated it was to be validated by comparing data generated by simulations to experimental data. Once the model was validated, the final goal was to use GT-Power to explore the abilities of cam phasing engines. By exploring all of the possible intake and exhaust cam angle pairs, the optimum position would be chosen while trying to maximize specific quantities. The target parameters include volumetric efficiency, fuel efficiency, indicated mean effective pressure (IMEP) and residual exhaust gases.

3.2. Mapping an Engine

In the design process of an engine, the physical layout of the engine has several important characteristics. These include the number of cylinders, the number of valves per cylinder, the displacement and the compression ratio. The bore and stroke of an

engine determine the displacement of each cylinder. The geometry of the piston crown also has a major effect on the properties of the combustion.

Once these parameters have been chosen, several other parameters must still be optimized. The fuel delivery and spark timing must be adjusted based on the engine's operating conditions. An engine's operating conditions are defined as the engine's rotational speed and the engine's load. The load on an engine is the amount of torque the engine produces. Because an engine is run almost always at a stoichiometric ratio of air and fuel, the number of moles of air inducted could be used. Instead of the number of moles of air inducted, the pressure of the intake manifold (which can be easily related to the number of moles) is more commonly used.

The optimized values of spark timing and fuel delivery for every possible engine operating condition are called an engine map. These values are then placed into a lookup table where they can be retrieved by the engine control unit. An engine with intake and exhaust cam phasing, however, has two additional values that must be determined for every operating condition. Adding these two parameters significantly increases the amount of testing required to create an optimized engine map.

Most engine testing is performed on an engine dynamometer. An engine dynamometer is able to very accurately control the rotational speed of an engine and therefore able to capture data at any engine speed. The whole range of possible engine speeds needs to be mapped, so the engine speeds that are analyzed range from idle to the engine's red line speed. This range of engine speeds is discretized so that data is taken about every 50 or 100 rpm.

At each engine speed, the load is varied by controlling the throttle's position. Again the whole range of loads must be analyzed, so data is collected at throttle positions ranging from closed throttle to wide open throttle (WOT). All of the remaining parameters such as spark timing must be tested at each coordinate on the two dimensional space of engine speed and load. Depending on the operating condition one value of each parameter is chosen. For example at idle speed with no load, the spark timing that produces the lowest emission and most stable combustion would be chosen.

3.3 Engine Setup

All testing was performed at The Ohio State University's Center for Automotive Research in an engine dynamometer test cell. The testing was performed on a modern 2.2 liter four cylinder gasoline preproduction engine. The fuel is port injected and spark ignited. Both the intake and exhaust cam timing can be controlled independently with a 15 CAM degree range. A picture of the engine is shown in Figure 13. Because it was a preproduction engine, its prototype calibration varied slightly from the production one. In addition several physical modifications were made to the engine. The radiator and cooling system were removed and replaced with a liquid water heating system. To provide a consistent source of air, the intake system was attached to a 50 gallon drum that draws room temperature air.

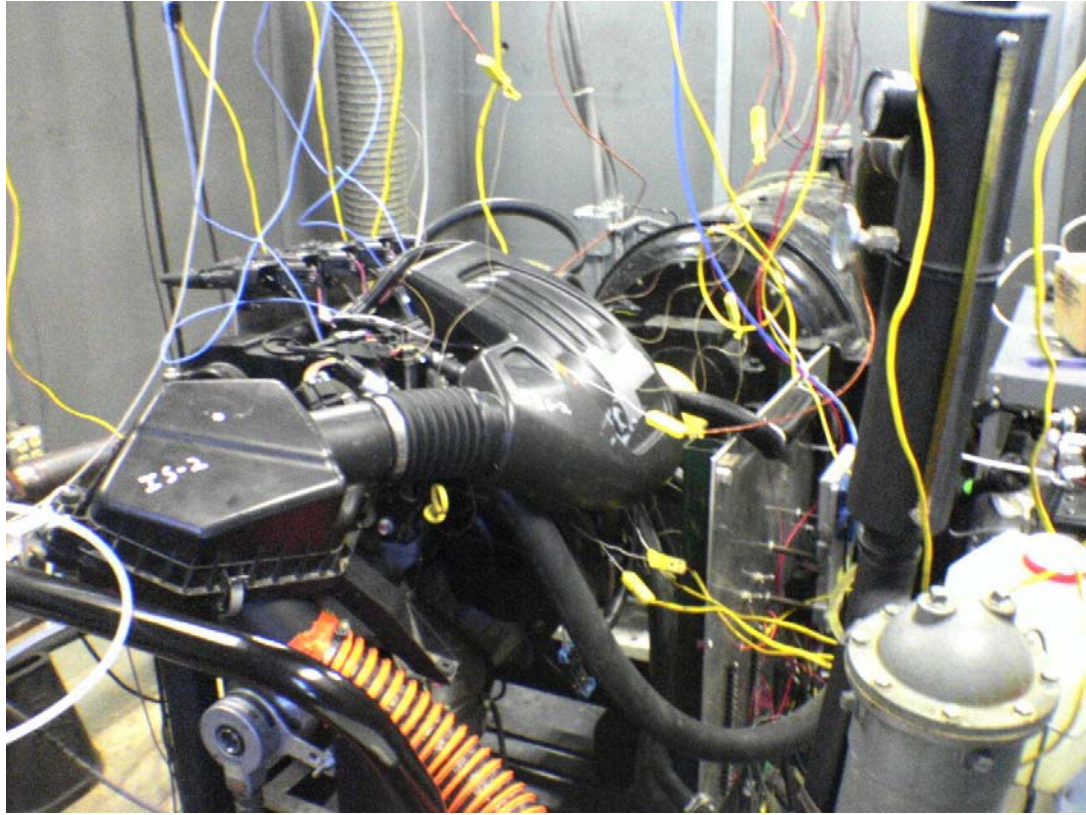


Figure 13: Picture of the Engine Experimental Setup

In addition to these modifications, many other components were instrumented so that data could be collected. A laminar flow sensor was attached to the entrance of the intake manifold to measure the mass flow rate of the air entering the intake. Two pressure sensors were placed in the intake system. One measures the ambient pressure and the other measures the manifold air pressure. The intake system was also outfitted with several thermal couples to provide a temperature distribution for the intake. Each runner in the intake manifold had two thermal couples to measure the wall temperature and air charge temperature. Another set of thermocouples was placed to measure the pre- and post-throttle temperatures. The exhaust system was also outfitted with several thermocouples. Another important modification to the exhaust is the addition of multiple heated exhaust gas oxygen sensors (HEGO) and universal exhaust gas oxygen sensors.

Additionally, a high precision angle displacement sensor with a one degree resolution was added to the crankshaft. The dynamometer measures the engine speed, torque output and power output. To measure the in-cylinder pressure, a special spark plug with a built-in pressure sensor was used. The data acquisition for the pressure sensor was triggered by the crank angle sensor such that a pressure measurement was taken every crank angle degree. On the exhaust side, a Horiba was used to analyze the emissions and determine the composition of the gases.

Excluding the in-cylinder pressure sensors, the data was acquired at 100 Hz through a 12 bit data acquisition system. The interface used for this was Labview version 7. On the controller side, an ETAS system was used. ETAS is a sophisticated control computer which directly allows the monitoring and adjustment of many control parameters inside the ECU of the engine. With ETAS both the intake and exhaust cam timings could all be controlled. Although ETAS can control other parameters such as spark timing, all other parameters were left unchanged. This uniformity provided the basis for determining the effects of cam phasing on combustion.

3.4 Experimental Procedure

As previously stated, the goal of the testing was to determine the impact of intake cam timing, exhaust cam timing, engine speed and manifold air pressure on combustion. Because time is a major constraint, the testing points were chosen in a semi-random manner such that the whole range of engine conditions was covered with a relatively low number of points. The data set collected is sparse in the four dimensional parameter space yet it is space filling. Each operation point, which consisted of distinct values for the four parameters discussed earlier, was allowed to reach steady state after which thirty

seconds of data was taken. The data was then averaged for each of the operating points. For the in-cylinder pressure data, 200 cycles of data was collected and the data was averaged for each crank angle degree.

A total of 422 operating points were chosen to best represent the most encountered engine conditions. The engine speed ranged from 1000 to 3500 rpm and the manifold air pressure ranged from 0.2 to 1 bar. Both the intake and the exhaust cams had a range of 0 to 50 crank angle degrees. The step sizes for the operating conditions were 200 rpm, 4 crank angle degrees and 2 degrees of throttle angle. Because the manifold air pressure was controlled with the throttle angle, the manifold air pressure was not limited to a discrete set of values. Figure 14 shows the distribution of the operation points in four two-dimensional projections.

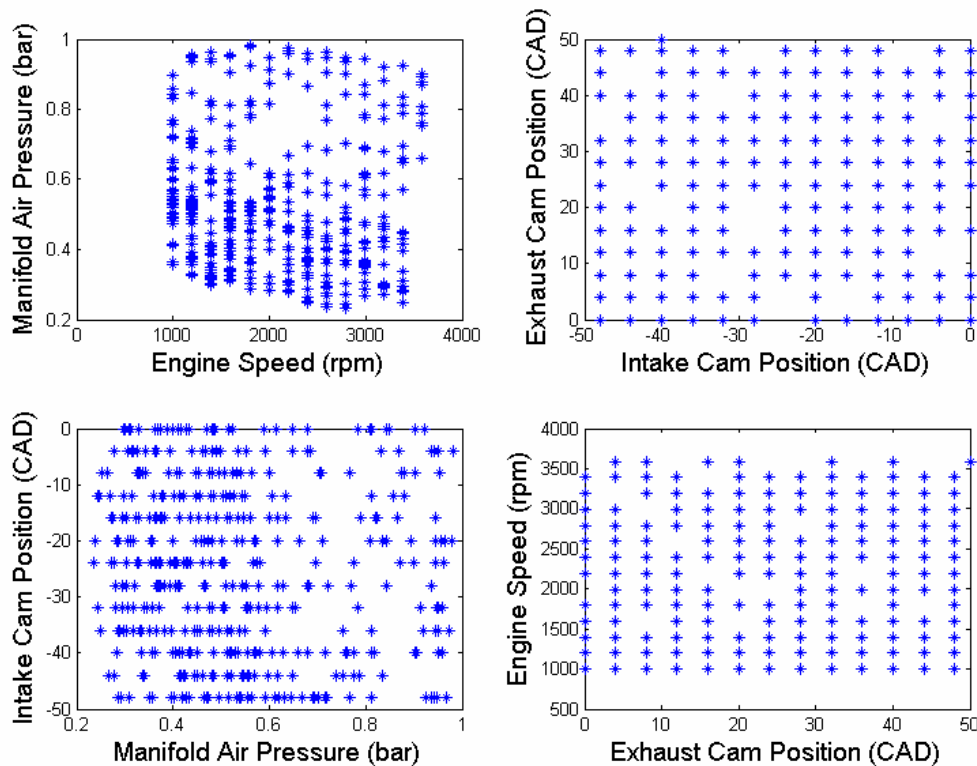


Figure 14: Distribution of Operating Points

3.5 Engine Simulations

Instead of testing every operating point on a dynamometer, a computer model of an engine is used to simulate the engine. One program used to simulate an engine is Gamma Technology's GT-Power. Like most engine simulations, the physical dimensions of the complete powertrain system must be entered. The process of creating a GT-Power model begins with dividing the powertrain into its components. The major components of the powertrain are the throttle, the intake manifold, the fuel injectors, the engine, the exhaust system and the catalyst. To model the intake manifold, the most important aspect is to model all of the pipe bends and flow splits. GT-Power has preset components for straight pipes, bent pipes and flow splits. Each component is defined by several parameters such as discharge coefficients, cross sectional area and lengths.

In addition to the physical properties of the engine, a combustion model must be entered. The flow dynamics created from the opening and closing of the intake and exhaust valves are complex. Therefore it is difficult to replicate the intricate mixing action of fuel using a simple model. If the intake valves of an engine have a staggered opening, then a rotation about the centerline of the cylinder called swirl is created. Depending on the location of the intake valves and the rate at which they are opened another mixing action called tumble may occur. Instead of rotating about the centerline of the cylinder, tumble rotates about the diameter of the cylinder. Combustion is largely dependent upon the mixing inside the cylinders and the local air/fuel ratio around the spark plug. Therefore, the in-cylinder flows are very important. Although it is possible to create a model that truly captures all of the fluid motion, the model would take a significantly longer time to converge to a solution. A long convergence time is

unfavorable, so a combustion model is inputted. Using a combustion model reduces the simulation time and accounts for the in-cylinder fluid motion.

3.6 How GT-Power Generates a Solution

GT-Power is based on one-dimensional gas dynamics which account for fluid flows and heat transfer. Each component in a GT-Power model is discretized or separated in many smaller components. These subcomponents have very small volumes and the fluid's scalar properties in these volumes are assumed to be constant. The scalar properties of a fluid include pressure, temperature, density and internal energy. Each volume also has vector properties that can be transferred across its boundaries. These properties include mass flux and fluid velocity. Figure 15 illustrates the difference between vector and scalar properties. GT-Power determines the change in the scalar properties by solving simultaneous one-dimensional equation.

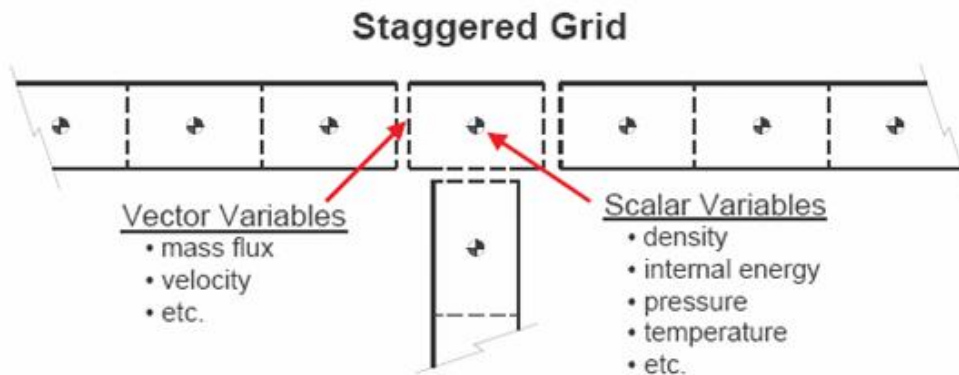


Figure 15: Illustration of Component Discretization (GT-Power Manual, 2004)

The first equation ensures the conservation of mass as seen in Equation 1. Related to the mass equation is the conservation of momentum relationship as seen in Equation 2. From these two equations the trapped air and residuals masses can be found. The equations are also used to determine the fuel dynamics and mass flow rates. GT-

Power also uses Equation 3 which ensures that energy is conserved. The final equation is an exergy balance as shown in Equation 4 which is implicitly solved. Using these equations, the heat transfer from a volume to the walls or another volume can be determined.

$$\frac{dm}{dt} = \sum_{boundaries} m_{flux}$$

Equation 1: Mass Continuity Equation

$$\frac{d(m_{flux})}{dt} = \frac{dpA + \sum_{boundaries} (m_{flux} u) - 4C_f \frac{\rho u^2}{2} \frac{dxA}{D} - C_p \left(\frac{1}{2} \rho u^2 \right) A}{dx}$$

Equation 2: Conservation of Momentum Equation

$$\frac{d(me)}{dt} = p \frac{dV}{dt} + \sum_{boundaries} m_{flux} H - h_g A (T_{gas} - T_{wall})$$

Equation 3: Conservation of Energy Equation

$$\frac{d(\rho HV)}{dt} = \sum_{boundaries} (\rho u A_{eff} H) + V \frac{dp}{dt} - h_g A (T_{gas} - T_{wall})$$

Equation 4: Implicitly Solved Exergy Equation

3.7 GT-Power Model Creation

In broad terms, a model is created using two types of discretization. Firstly, the complete powertrain system is grouped into general components. These components consist of air cleaners, valves, piping, valves, fuel injectors, mufflers, resonators, catalytic converters, combustion chambers, resonators and if applicable turbo/intercoolers. The second aspect is separating each component into multiple control volumes. Each control volume is bounded by another control volume or wall. By

discretizing the system into sufficiently small volumes, the properties of the fluid in that volume can be assumed to be constant.

GT-Power is an object oriented program with a logical user interface. To create a model, components are placed on a worksheet. Components are connected using lines to mirror the fluid paths. This process is similar to creating a block diagram or Simulink model. Figure 16 shows an example of difference components that are used to create a model and how they are connected. Several parameters must be entered into each component to specifically reflect the physical engine. To define these values, a user must double click on the object and enter the required values in a graphic user interface window. A picture of this window is shown in Figure 17. The information that must be entered for each component will be described in the next sections.

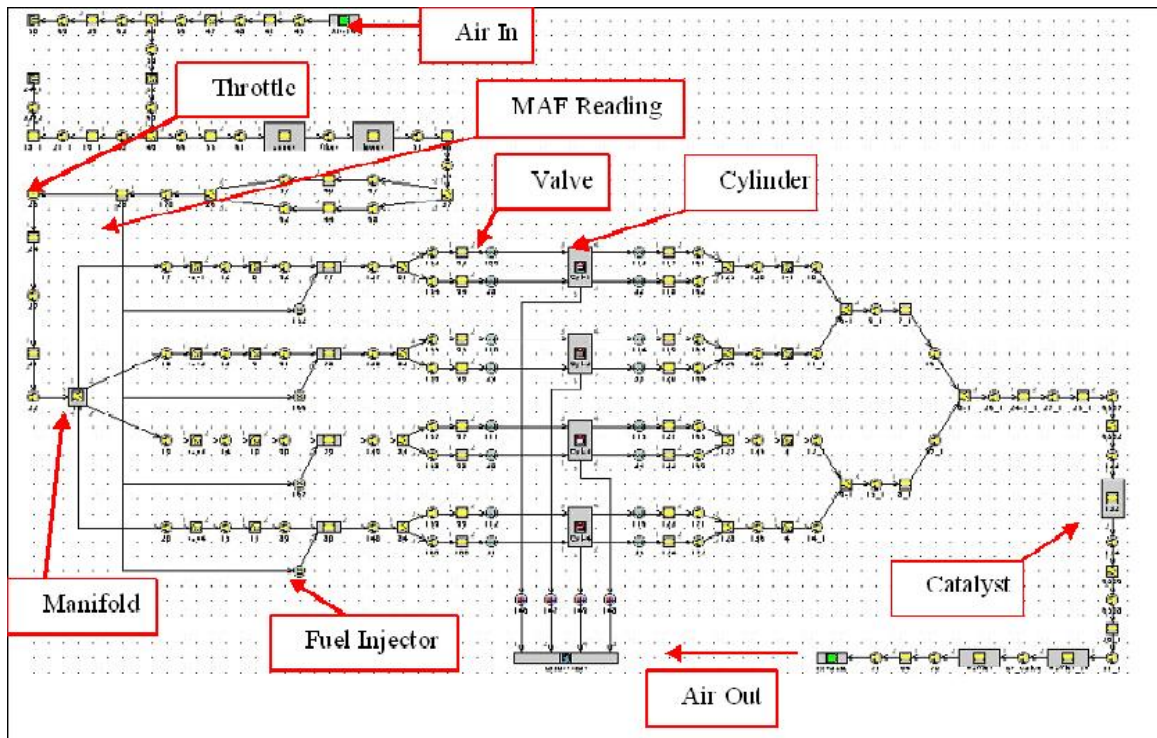


Figure 16: Example of a GT-Power Model

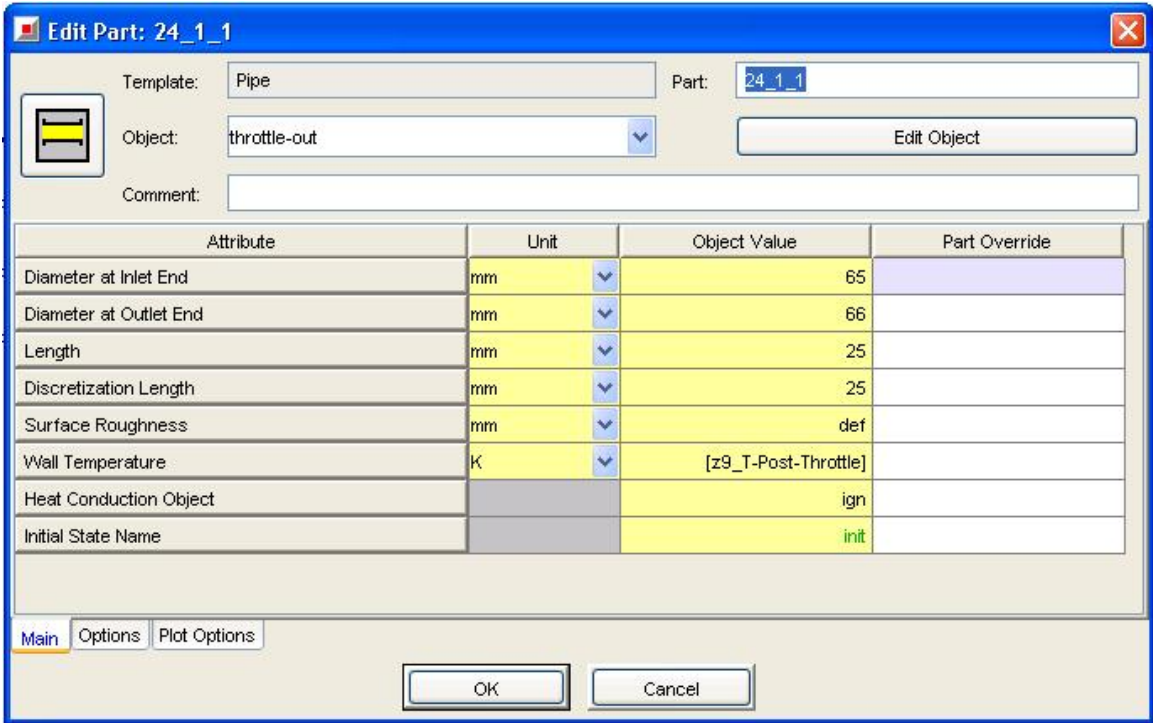


Figure 17: Part Definition Window

3.7.1 Ambient Air Volume

Since it is easiest to discuss the parts in their fluid path order that is how they are presented. To begin, an air mass must be generated to simulate the ambient conditions. The air mass is an infinite volume of gas with uniform properties. The pressure, temperature and gas composition must be specified. Atmospheric pressure and temperature as well as standard air composition (76.7% N₂ and 23.3% O₂) were used for all simulations. With this set of conditions, no purities are present so an air filter is not needed.

3.7.2 Lumped Throttle

In a physical engine the ambient air passes through a set of piping that guide the air through an air filter and eventually through a throttle. However in the model of the engine, all of these components were lumped into a single component. One of the goals of

this model was to minimize the simulation type. Experimentally it was found that the simulation times were significantly reduced with a lumped throttle. In terms of ECU, most of the engine control is based on the intake manifold pressure not the throttle position. For this reason the throttle was viewed just as a flow restriction with a variable discharge coefficient. The relationship between the discharge coefficient and the intake manifold pressure was determined by running a series of simulations in GT-Power. For these simulations random discharge coefficients ranging from 0.005 to 0.9 were tested. By using the manifold pressure that resulted from the simulation, a relationship between the discharge coefficient and the manifold pressure was found.

3.7.3 Piping for the Intake and Exhaust Systems

Modeling the intake and exhaust manifold was straight forward. GT-Power splits piping into straight pipes, curved pipes, flow splits, orifices and end caps. To define a straight pipe the actual length, inlet area (or diameter), outlet area (or diameter), surface roughness and wall temperature must be specified. In addition the discretization length which was previously discussed must also be provided. The discretization length was 3 centimeters for the intake system and 5 for the exhaust. Curved pipes have the same properties as a straight pipe with the addition of a radius of curvature and curvature angle. Flow splits are defined by a volume, surface roughness and wall temperature. Anytime the diameter of the pipe changes or the flow is impeded an orifice element must be placed. An orifice is defined by a discharge coefficient and a diameter.

GT-Power has special pipe objects like throttles, mufflers and catalytic converters. As previously stated a throttle was not used to reduce the computation time. Similarly a muffler and catalytic converter were also not used. Instead they were

represented as an orifice and pipe. Emission and after-treatment was not a major consideration for this project, so a catalyst is not necessary.

3.7.4 Fuel Injectors

The final components before the engine head is the fuel injectors. Fuel injectors are specified by an air/fuel ratio, a fuel delivery rate, a fuel temperature, injection timing and a fuel vapor fraction. For all of the simulations the air/fuel ratio was set to stoichiometric. The fuel injectors are connected to the intake ports and can simulate the wall wetting dynamics. Not all of the fuel that enters combustion chamber is gaseous. A fraction of the fuel is liquid. This fraction is related to the mass of fuel that puddles in the intake ports.

3.7.5 Intake and Exhaust Cam Profiles

The profiles on a cam shaft are difficult to quantify, so GT-Power ignores them. Instead, the valve lift that the cam profiles produces is used. The valve lift must be tabulated as a function of crank angle. In addition the discharge coefficient must be tabulated as a function of valve lift. With these values the volumetric flow rate and friction loss can be calculated. Like the intake and exhaust system, the discharge coefficients can be found using a flow bench.

3.7.6 Engine Block

The engine block is the most complex component to model. The typical dimensions of an engine like bore, stroke, compression ratio, connecting rod length and clearance height must be entered. In addition, the physical dimensions of the head, piston and rings needs to be included. The inertia of the crankshaft and information on the cooling system are also required. Finally, GT-Power needs a combustion model. A

major section of this thesis will be devoted to the creation of a combustion model. Combining all of the parts, a GT- Power model like Figure 18 is created.

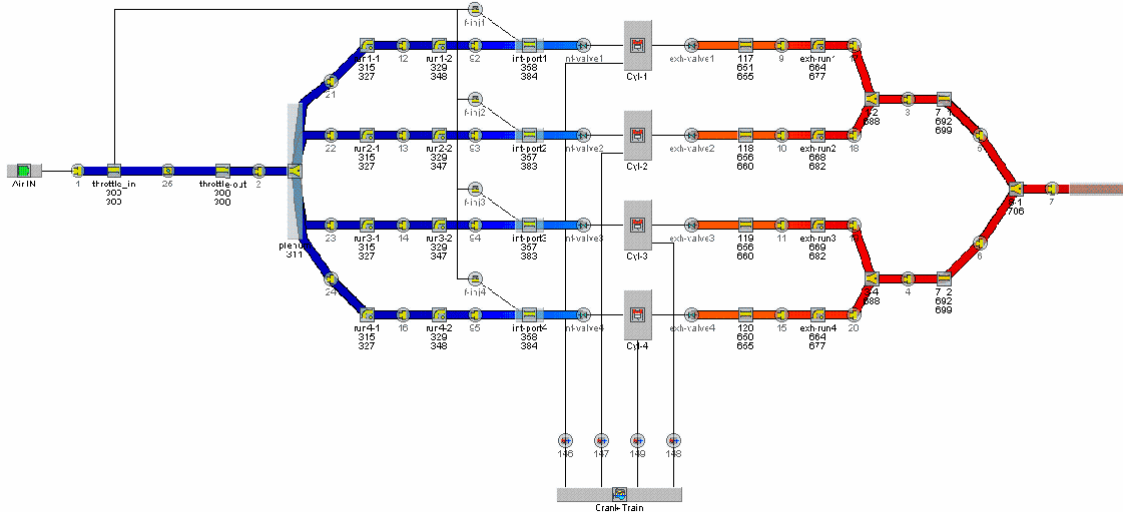


Figure 18: Final GT-Power Model

3.8 Engine Model Validation

After a complete model is created, the model must be compared with experimental data and validated. To ensure that the model accurately represents the powertrain system, the parameters are tuned. The same data cannot be used for creating the model and validating it. Data used for creating the regression would automatically have a high correlation. Therefore the data used to validate the engine model was independently collected from the data used to create the model. A correctly calibrated model will create accurate results that are very reproducible. Unlike a normal engine that has variation errors, a model only has modeling and calibration errors. Once the model is validated, any operating condition can be run, even operating points that could be dangerous to run on a real engine.

Chapter 4: Data Analysis

4.1 Combustion Modeling

The most common method of defining combustion is with a mass fraction burned curve. Mass fraction burned is the ratio of the cumulative heat release to the total heat release as shown in Equation 5.

$$MFB(\theta) = \frac{\int_0^{\theta} \frac{dQ}{d\theta}}{Q}$$

Equation 5: Mass Fraction Burned Equation

The mass fraction burned is also defined as the ratio of the apparent heat release to the lower heating value as shown in Equation 6. Therefore if the mass fraction burned is known as a function of crank angle, then the apparent heat release can be approximated.

$$MFB = \frac{Q_{apparent}}{Q_{LHV}}$$

Equation 6: Mass Fraction Burned Relationship to Apparent Heat Release

When the mass fraction burned is graphed against crank angle degrees, the curve can be described using a Wiebe function. Equation 7 shows the form of a Wiebe function.

$$MFB(\theta) = 1 - \exp \left[-a \left(\frac{\theta - \theta_0}{\Delta\theta} \right)^{m+1} \right]$$

Equation 7: Wiebe Approximation of Mass Fraction Burned Curve

In this equation, θ is crank angle degrees with θ_0 corresponding to the initialization of heat release and $\Delta\theta$ corresponding to the duration of burn. The equation is also defined by two constants a and m which have typical values of 5 and 3 respectively. Because the

expression is one minus the inverse of an exponential term, the mass fraction burned is limited to values between zero and one as expected. A sample Wiebe curve is plotted in Figure 19.

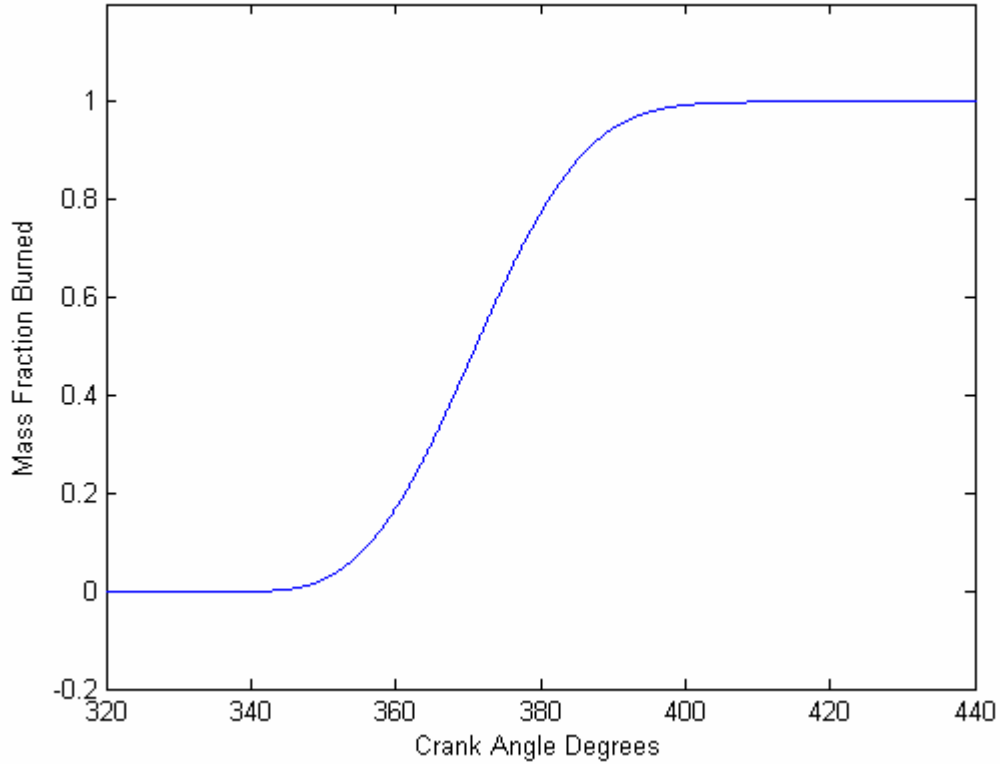


Figure 19: Representative Wiebe Curve

4.2 Differences in Combustion between Conventional and Cam Phasing Engines

For conventional engines under operating conditions where the combustion is stable, the combustion model has relatively little variation. Therefore the values of the coefficients a and m could be assumed to be constant for all operating conditions with stable or “good” combustion. Although this will not yield perfect results, it would produce relatively accurate results.

One of the reasons the mass fraction burned curve stays unchanged is because the dynamics of the engine change only very slightly from operating point to operating point. At higher engine speeds the combustion occurs more rapidly but maintains a constant burn rate with respect to crank angle degrees. When the load is increased, more fuel and air are added to the combustion chamber, but their ratio is still nearly stoichiometric. Therefore as long as the fuel does not auto-ignite, the combustion properties remain essentially the same. All of these factors, however, are dependent on unchanging valve timing.

Engines with cam phasing have changing valve timing and can have drastically different flow patterns. The largest factor is the variation in valve overlap. Valve overlap is the region when both the intake and exhaust valves are open. When valve overlap is changed, the flow patterns are heavily changed. Normal valve overlap prevents a certain portion of the exhaust gases from leaving the combustion chamber. This leftover exhaust gas is called residual exhaust gas. However in cases where the valve overlap is very large, the direction of the exhaust flow is altered. The pressure inside the intake manifold is considerably lower than the exhaust manifold, so the pressure gradient reverses the flow. Instead of the combustion gasses flowing into the exhaust system, they flow into the intake. Finally once the exhaust valves close and the pressure inside the combustion chamber declines, the flow changes directions again. The combination of combustion gases and a fresh air charge is pulled back into the engine's cylinders. Combining the requirements of a higher number of testing points and a varying combustion model makes rapidly creating an engine map of an engine with cam phasing difficult.

4.3 Heat Release Calculations

Once all of the data was collected, the combustion's dependence on intake timing, exhaust timing, engine speed and manifold air pressure still needed to be found. Combustion was previously analyzed using a mass fraction burned curve, but no direct measurements of mass fraction burned were taken. Instead, the in-cylinder pressure measurements were recorded. Using Equation 8, the differential changes in volume and pressure can be related to the heat release rate.

$$\frac{dQ}{d\theta} = \frac{\gamma}{\gamma-1} p \frac{dV}{d\theta} + \frac{1}{\gamma-1} V \frac{dp}{d\theta}$$

Equation 8: Heat Release Rate as a Function of Volume and Pressure

In this equation γ is the specific heat ratio which has a constant value of 1.4. The pressure, p , is the in-cylinder pressure and V is the volume. Because all of the data triggered every crank angle degree, the differential volume and pressure values can be found using the finite difference approximation. The volume in the cylinders was never measured, but the dimensions of the engine are known. Using the connecting rod length, the radius of the cylinder and the compression ratio, the volume inside the combustion chamber can be related to the crank angle using Equation 9.

$$V = V_c \left(1 + 0.5(r_c - 1) \left(R + \cos(\theta - \pi) - \left(R^2 - (\sin(\theta - \pi))^2 \right)^{0.5} \right) \right)$$

Equation 9: Relationship between Volume and Crank Angle

The heat release rate generated from these equations is not a direct measure of the heat released by the fuel. Instead, this equation generates the apparent or net heat release. Because the gases inside the cylinders have different temperatures than the cylinder's walls, there is heat transfer between the gases and the walls. Before combustion, heat

flows from the walls to the gases; after combustion heat flows from the gases to the walls. The measured heat release rate is therefore the heat released by the fuel minus the heat transfer losses.

4.4 Mass Fraction Burned Curves

Once these calculations were made for each cylinder, the values of the four cylinders were averaged. The resulting average mass fraction burn values were graphed against crank angle degrees and analyzed. Across the operation conditions, the mass fraction burned curves varied dramatically as shown in Figure 20. Upon first look, the greatest variation appears to be in the start of combustion. The start of combustion ranges from about 340 to 360 crank angle degrees. More interesting is the sharp changes in the heat release rates. To better illustrate this, Figure 21 shows a comparison between a representative mass fraction burned curve observed and one that is typical for a conventional engine. The mass burn fraction curve on the left (conventional engine) is very smooth and has only one inflection point. Conversely, the mass fraction burned curve of the engine with cam phasing (right graph) has a very abrupt change its curve and three inflection points. For the first part of the curve, the heat release is very rapid, but after only a short burn duration the heat release rate slows substantially.

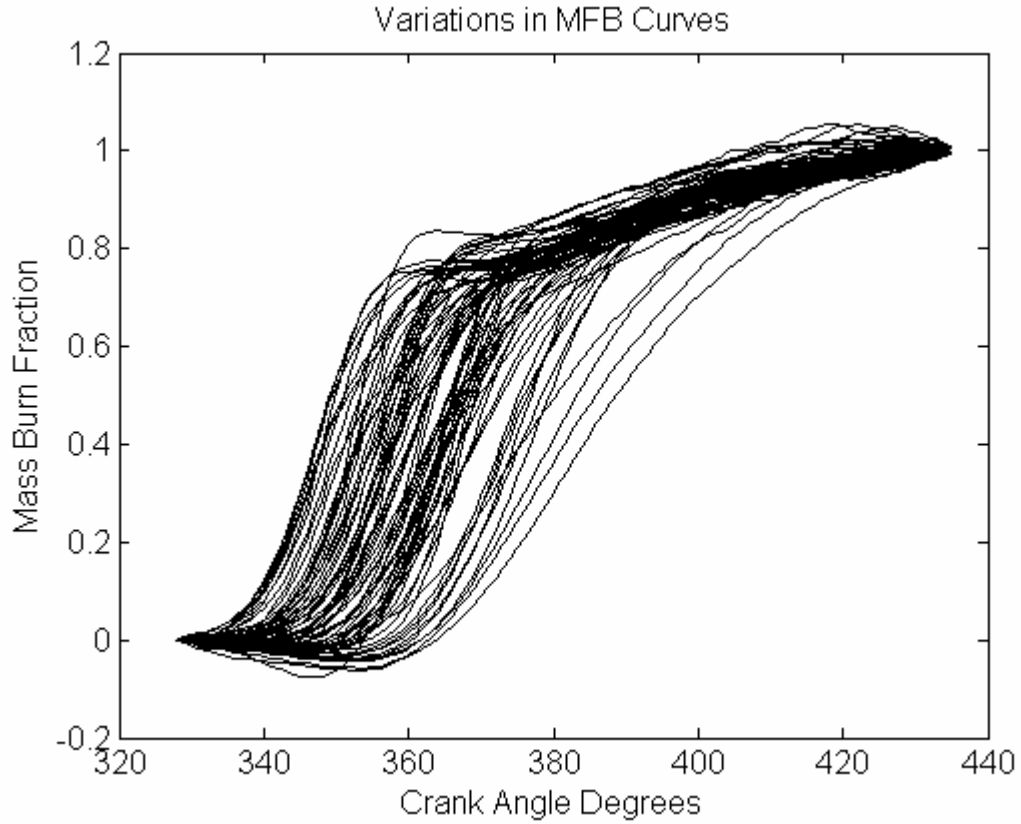


Figure 20: Variation in Mass Fraction Burned Curves

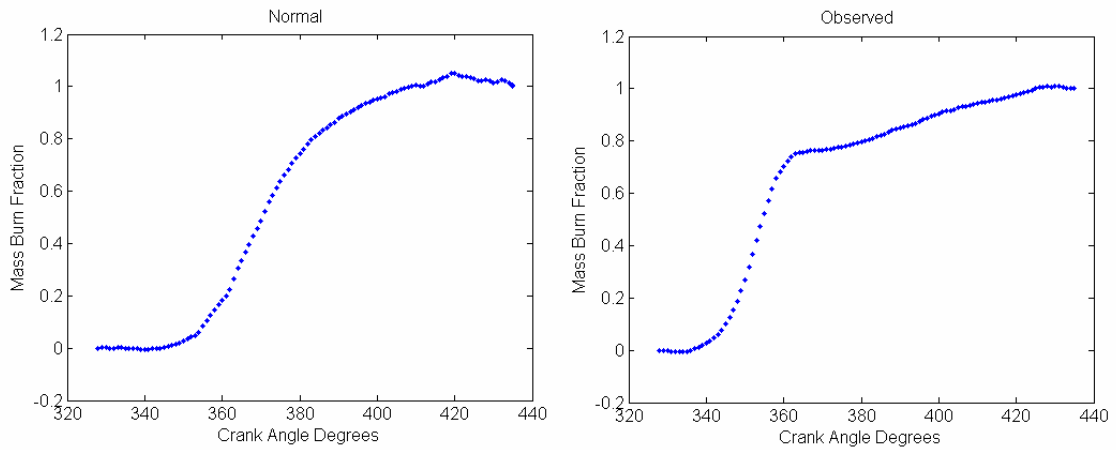


Figure 21: Representative Mass Fraction Burned Curve Comparison

This behavior is believed to be linked to heavy valve overlap. Because the valves overlap so much, the ratio of fresh charge to recirculated combustion products is very

low. This mixture is able to burn quickly but as the fuel is burned the oxygen becomes scarce. Without an adequate amount of oxygen, the burn rate is reduced. Depending on the operating conditions, this two tiered burning could be beneficial. Although the combustion may appear to be unstable and have some degree of auto-ignition, the combustion is very well behaved. Figure 22 shows a sample pressure trace of this type of combustion. If the combustion was abnormal, then the pressure trace would be very jagged. As seen by the graph, the pressure trace is very regular.

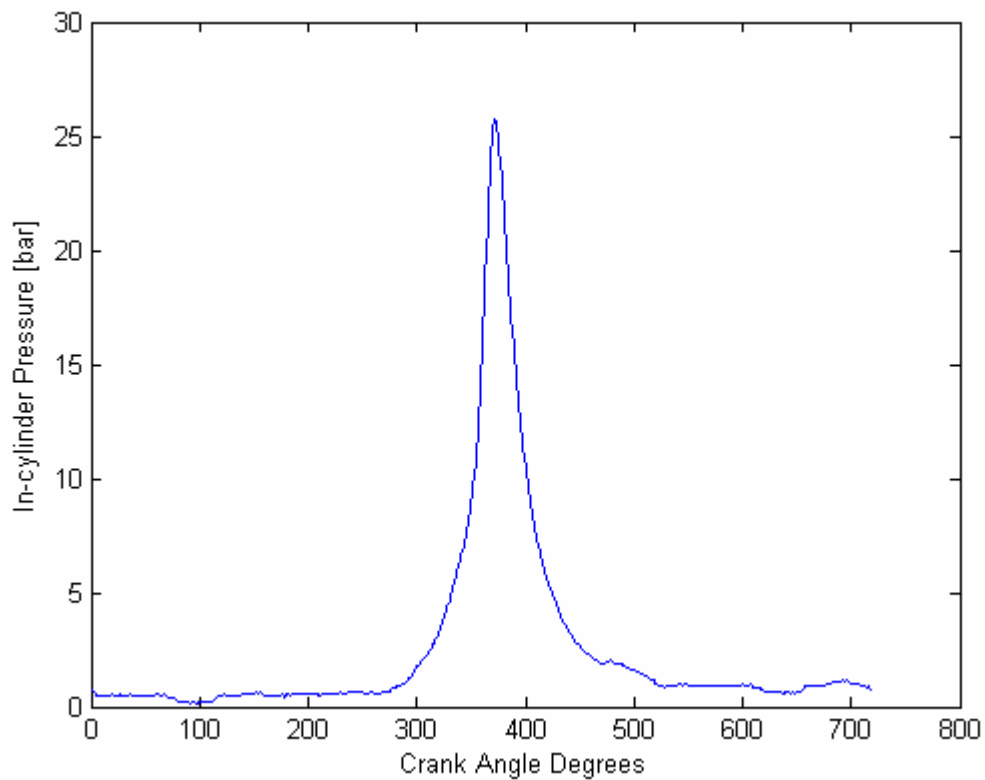


Figure 22: In-cylinder Pressure Trace of Two Mode Combustion

4.5 Modeling Difficulties of Mass Fraction Burn Curves

After creating all of the mass fraction burned curves, two problems were immediately apparent. First, the variation in the curves means that the coefficients of a

Wiebe approximation would not be constant. Secondly because the combustion had two modes, a Wiebe approximation would not be a very accurate representation of the combustion. A dual mode combustion mass fraction burned curve is shown in Figure 23 along with its best fit to a Wiebe approximation. The Wiebe curve fit inadequately models combustion with more than one mode. To determine the best way to model the data, the curve was separated into two parts. The first section burns with an abundance of oxygen and should resemble a Wiebe curve. For the second half of the curve, the combustion is very slow and is nearly linear in many cases.

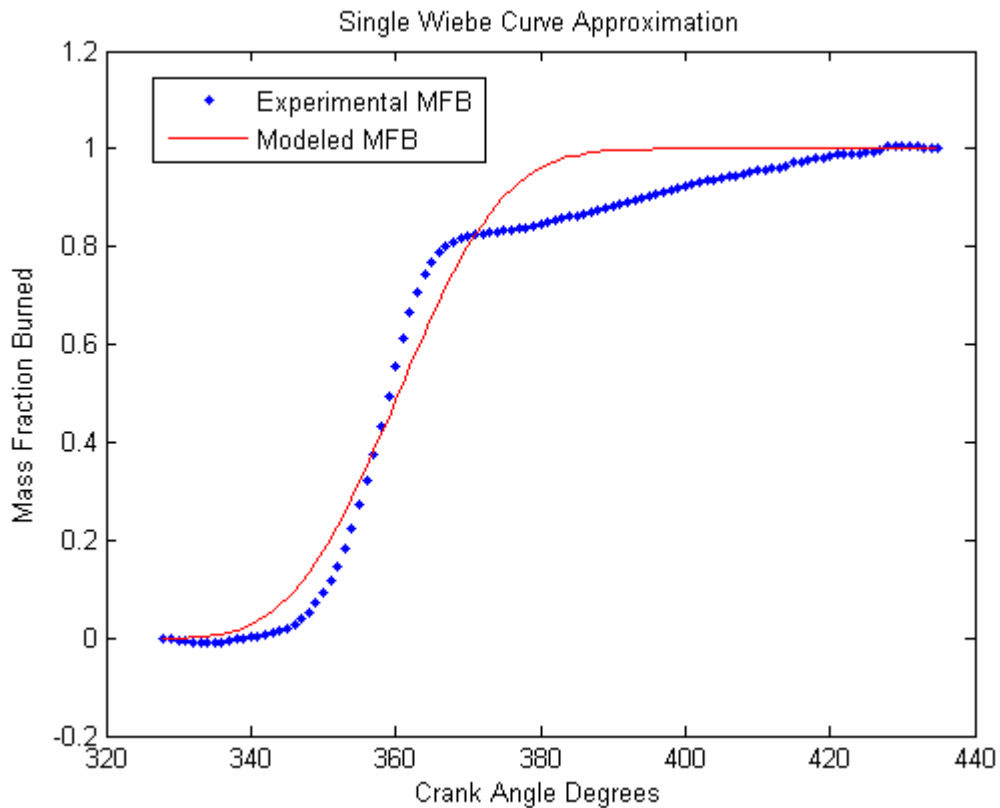


Figure 23: Experimental Data fit to a Wiebe Approximation

Initially a piecewise function was considered, but any discontinuities might cause problems. Instead of using a piecewise function, a summation of two Wiebe functions was considered. The beginning of the combustion resembled a Wiebe curve and given

the right coefficients a Wiebe curve can be relatively linear. To ensure that the maximum value was still one, a scale factor was used. The equation used to fit the two mode combustion data is shown in Equation 10.

$$MFB(\theta) = x \left(1 - \exp \left[-a_1 \left(\frac{\theta - \theta_0}{\Delta\theta} \right)^{m_1+1} \right] \right) + (1-x) \left(1 - \exp \left[-a_2 \left(\frac{\theta - \theta_0}{\Delta\theta} \right)^{m_2+1} \right] \right)$$

Equation 10: Mass Fraction Burned as a function of two Cascaded Wiebe Functions

Using this equation, the data and best curve fit had a strong correlation. Figure 24 shows the experimental mass fraction burned data and curve fit for a single operating condition. Compared to a single Wiebe approximation, a cascade of two Wiebe functions is seven times more accurate.

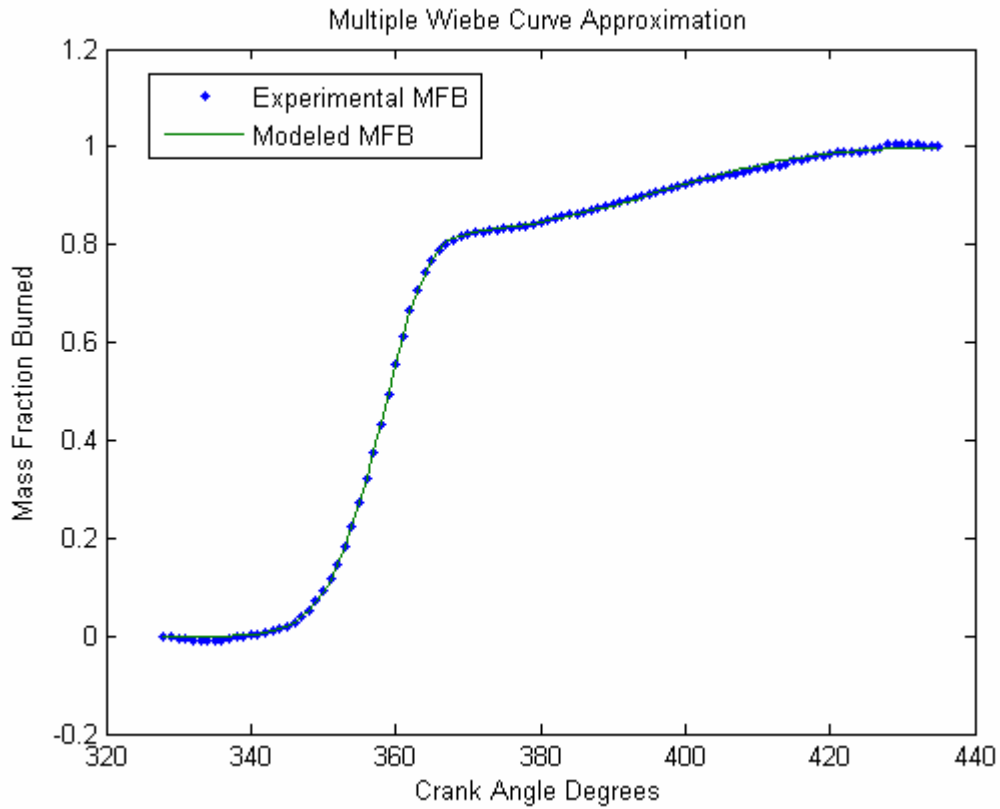


Figure 24: Mass Fraction Burned Data and Approximation Comparison

4.6 Variations in Mass Fraction Burned Approximation's Constants

Although the cascade of two Wiebe curves created an accurate approximation of the mass fraction burned curves for every condition, the constants in the approximation varied greatly. Instead of a value of around 5 for a single Wiebe function, the values of a_1 and a_2 in the two Wiebe approximation ranged from 10 to 2000 and 3 to 37 respectively. The values of the m constants also changed between the two types of approximations. The values of m_1 and m_2 ranged from 2 to 9 and 2 to 8 instead of about 3. The value of x , the scale factor, ranges from 0.5 to 0.9. Figure 25 shows the distribution of each of the five coefficients.

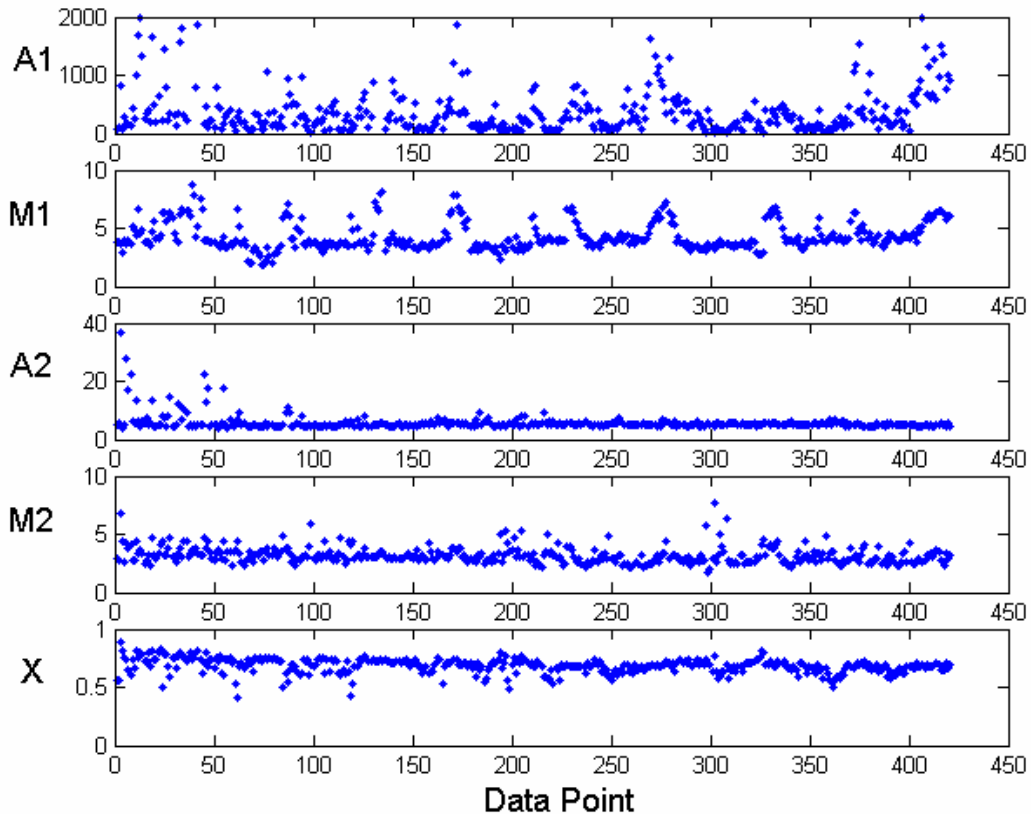


Figure 25: Variation in Mass Fraction Burned Approximation Coefficients

The problem with widely diffused data is that a constant value of each coefficient cannot be used. Figure 26 shows a comparison between the measured mass fraction curves and the approximation using the average coefficients' values. As apparent from the graph, constant coefficients cannot be used to represent the mass fraction burned across the operating conditions. Instead of constant coefficients, the coefficients must change with the operating conditions. To do this, a relationship between the operation conditions (engine speed, manifold air pressure, intake cam position and exhaust cam position) and the approximation's coefficients (a_1 , a_2 , m_1 , m_2 and x) must be found.

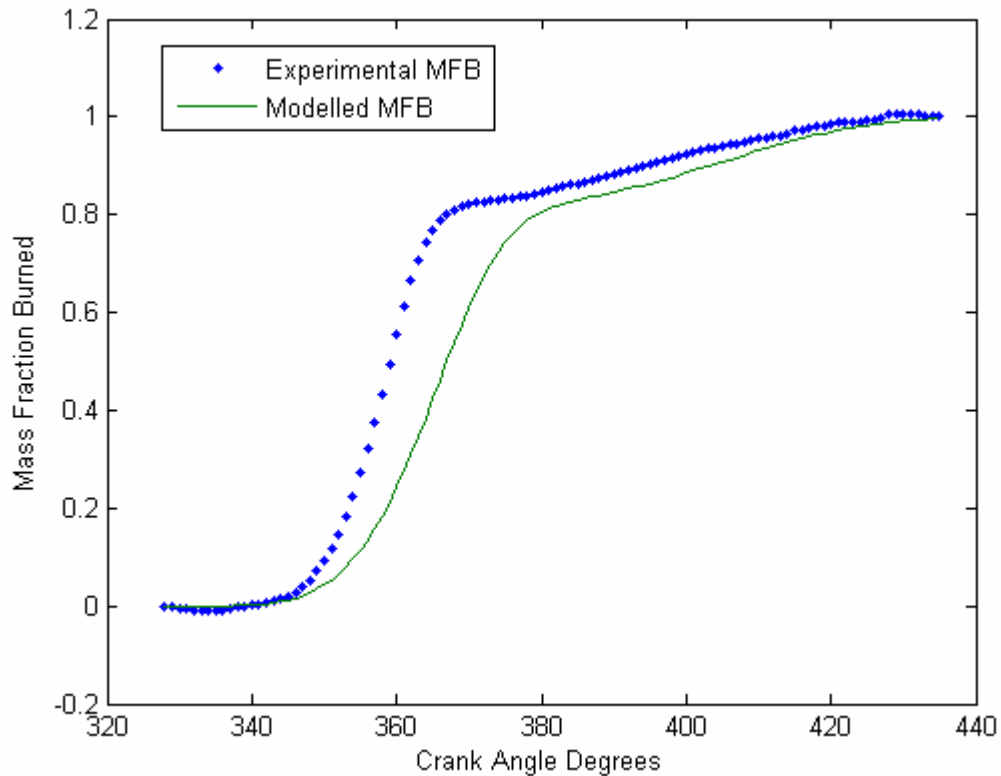


Figure 26: Comparison between Measured Mass Fraction Burned Curve and Approximation using the Average Coefficients

4.7 Coefficient Prediction Using a Step-wise Multivariable Regression

The method used to find this relationship was a step-wise multivariable regression. A step-wise multivariable regression is a stochastic method that is based on statistical probability. Experimental data is used to both determine the form of the equation and the coefficients of the terms. For the mass fraction burned approximation only linear and quadratic terms were considered. The first part of the step-wise multivariable regression was to determine which of the possible terms (4 linear and 10 quadratic) had a strong correlation with the output (coefficients of the mass fraction burned approximation). For the terms with a strong correlation, the coefficients were then found. Once all of the coefficients were found, the resulting equation should ideally be able to predict the coefficients of the mass fraction burned for any operation condition. This equation has the form of Equation 11.

$$\begin{aligned} F = & \alpha_1 \text{RPM} + \alpha_2 \text{MAP} + \alpha_3 \text{ICAM} + \alpha_4 \text{ECAM} + \alpha_5 \text{RPM} \times \text{MAP} + \alpha_6 \text{RPM} \times \text{ICAM} \\ & + \alpha_7 \text{RPM} \times \text{ECAM} + \alpha_8 \text{MAP} \times \text{ICAM} + \alpha_9 \text{MAP} \times \text{ECAM} + \alpha_{10} \text{ICAM} \times \text{ECAM} \\ & + \alpha_{11} \text{RPM}^2 + \alpha_{12} \text{MAP}^2 + \alpha_{13} \text{ICAM}^2 + \alpha_{14} \text{ECAM}^2 \end{aligned}$$

Equation 11: Equation Resulting from Step-wise Multivariable Regression

Because not all of the terms have a high correlation, some coefficients are zero. When determining the correlations, only 272 of the 422 data points were used. The other data points were set aside so the equation could be independently verified.

4.8 Results from Initial Regression

The initial step-wise multivariable regression provided results that were insufficiently representative of the mass fraction burned curve. The equations based on the operating conditions (intake cam position, exhaust cam position, MAP and engine speed) were unable to accurately predict the coefficients (a_1 , a_2 , m_1 , m_2 and x). A comparison of the coefficient of x found through optimization and predicted from the step-wise multivariable regression is shown in Figure 27. Also included in the graph is a residual of the fitted data. The R^2 correlation of the data was only 0.576. The target for the correlation value was at least 0.9. Approximating x using an average value would yield a similar error. The R^2 correlations of the other coefficients are also about 0.6. When the coefficients were used to try to predict the mass fraction burned curve, the results were also inadequate.

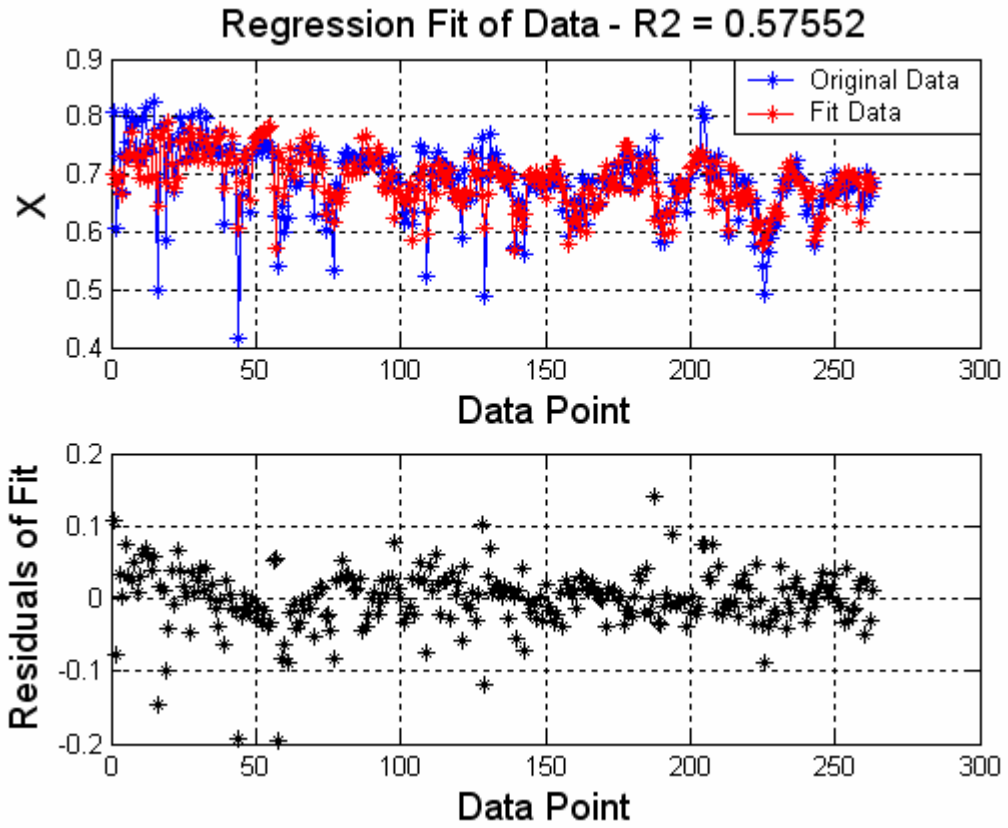


Figure 27: Comparison between Experimental and Approximated Values of Coefficient x

4.9 Grouping the Data into Regions

Knowing that the original step-wise multivariable regression produced inferior results, a new methodology would have to be used. Using data from the entire range of operating conditions did provide accurate results because there was too much variation in the coefficients. By separating the data into regions with less variation and then taking step-wise multivariable regression of each region should provide better results. It was initially believed that most important of the four operating condition was the engine speed and the MAP. After taking the first step-wise regression, it appeared that indeed the engine speed and MAP had a great influence on the values of the coefficients. Because these variables have the largest affect, the data was separated into nine regions in the engine speed versus MAP space. Organizing the data into any more than nine parts would spread the data too thin. The regressions would be poor because not enough data points could be used. When dividing the space into regions, the largest concern was keeping a relatively constant number of data points in each region. Figure 28 shows how the data was separated.

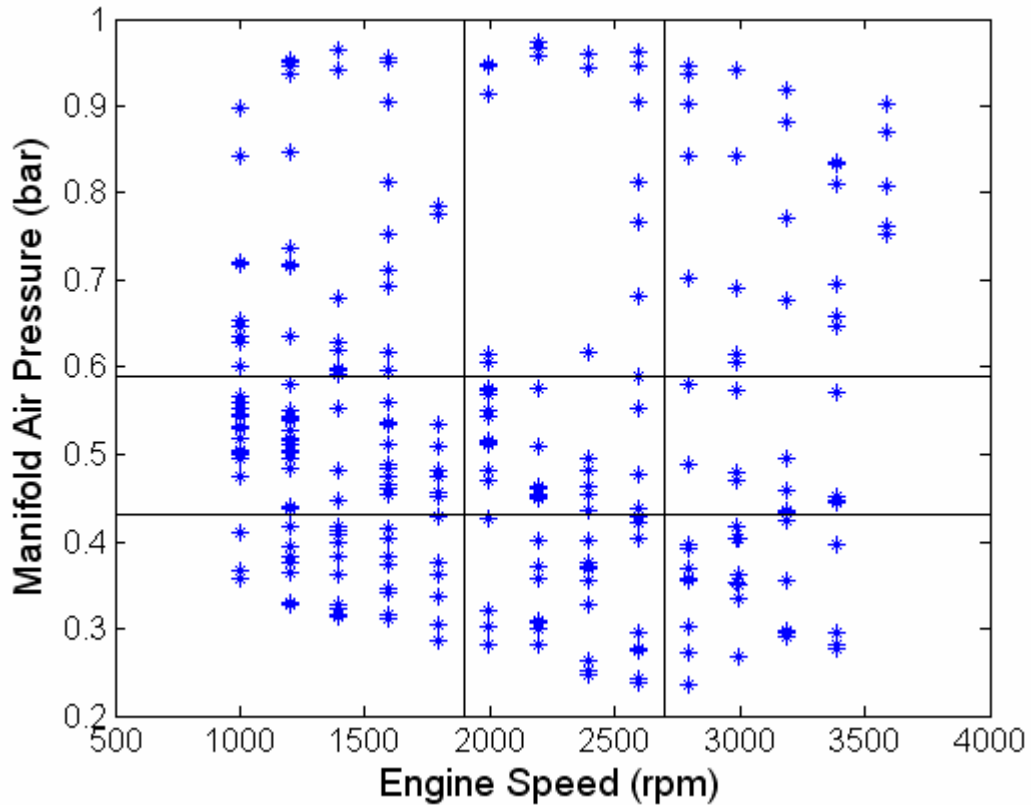


Figure 28: Boundaries for each Data's Region

After the data was divided into sections, step-wise multivariable regressions were taken of each region. The results were better than the regression taken over the whole region. The R^2 correlations varied between regions and coefficients but they ranged from about 0.7 to 0.9. A representative comparison of the data is shown in Figure 29. Separating the data into sections improved the regression's correlation, but the R^2 value was still low for most cases. Before the regressions were discarded as inaccurate, the predictive nature of the equations was tested. Although the regression does not have a remarkably high fit, the cascaded Wiebe approximation has a low sensitivity to the coefficients. Even though each of the coefficients differs slightly from the optimum

value, the results are very accurate when the coefficients are put into the mass fraction burned approximation.

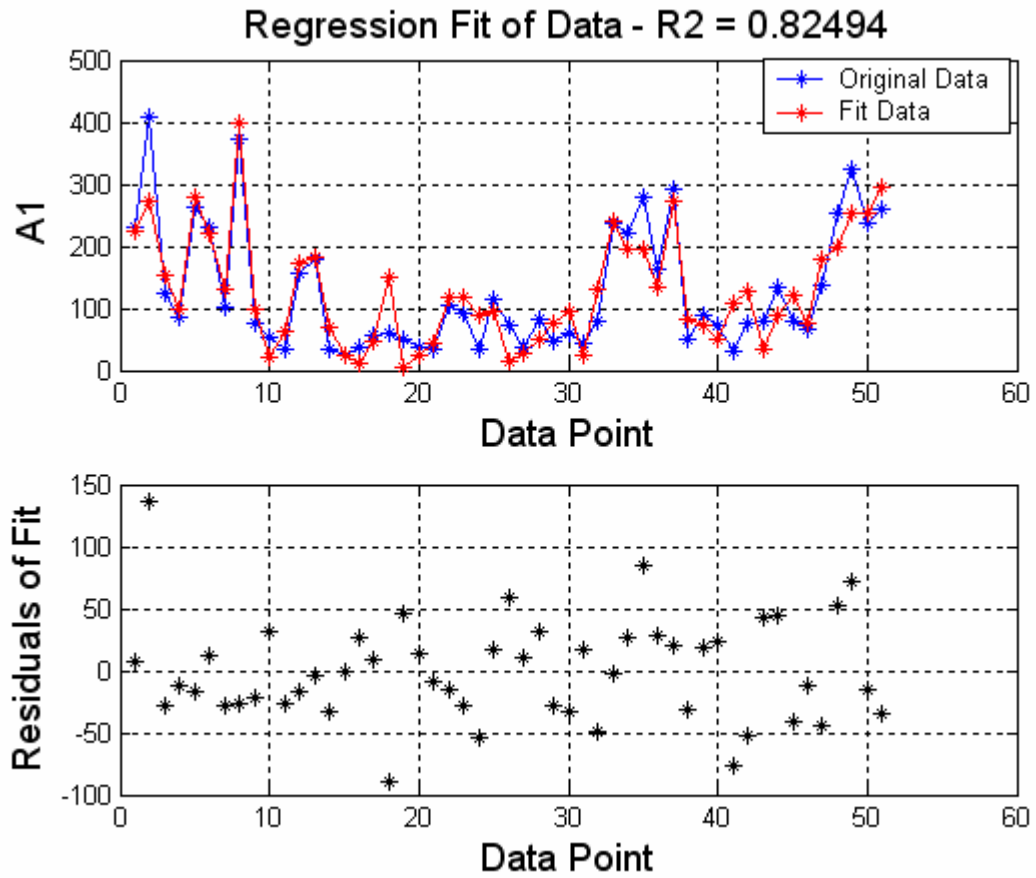


Figure 29: Comparison of Experimental and Approximated Values of $A1$

4.10 Predictive Ability of Regression Equations after Grouping

When verifying the predictive nature of the mass fraction burned approximations, data that was not used in regression was tested. The mass fraction burned curve generated from one set of regressions is compared to its experimental curve in Figure 30. Although there was some variation in the accuracy of the predictions, overall the fitting was very good. Compared to the approximation that used only one region, the approximation separated into nine regions had seven times less error.

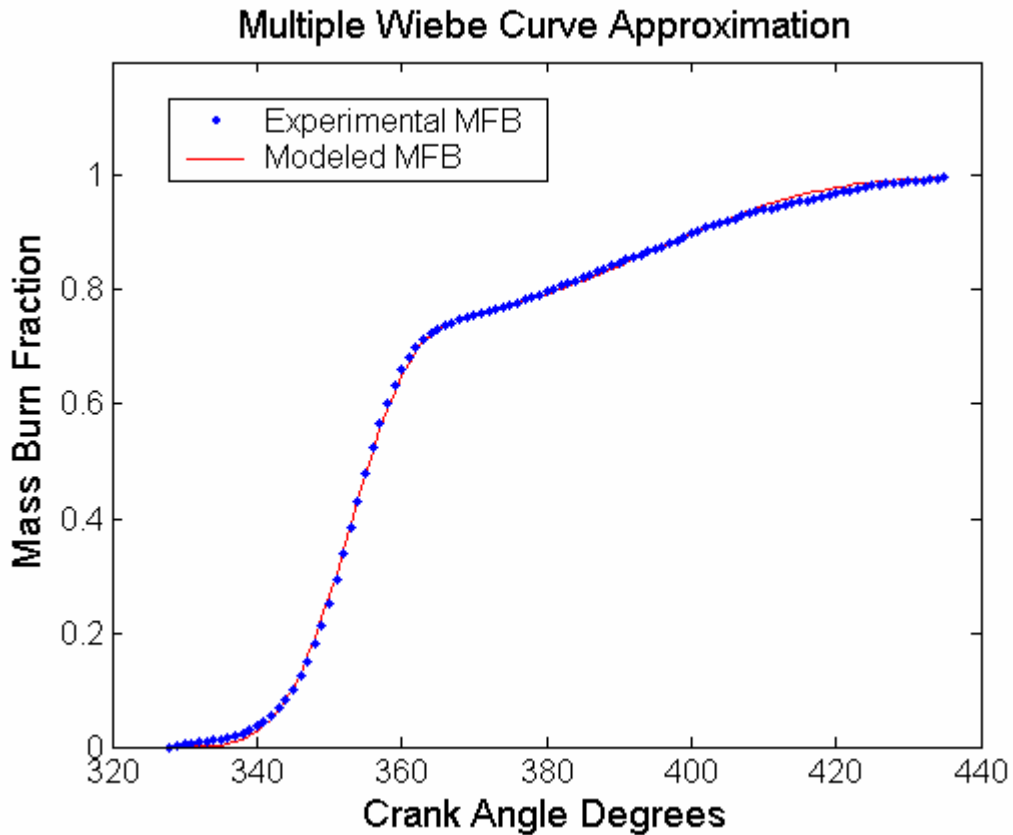


Figure 30: Comparison between Predicted and Experimental Mass Fraction Burned Curves

To calculate the error, the difference between the predicted and experimental mass fraction burned values at every point was taken. These values were then averaged for each operating condition. The average errors of different operating points were then

compared to find the average error and standard deviation of error for an entire region. These measures of error are shown in Figure 31. Across the regions the average error is around 0.02 and about the same for the standard deviation. The only regions with significantly higher error are the two regions corresponding to low engine speed with moderate or high MAP. Although the error is high, these regions are infrequently encountered. Except on a dynamometer, it is very difficult to have a low engine speed and a high manifold pressure. When it does occur, it stays at that condition for an exceptionally brief time.

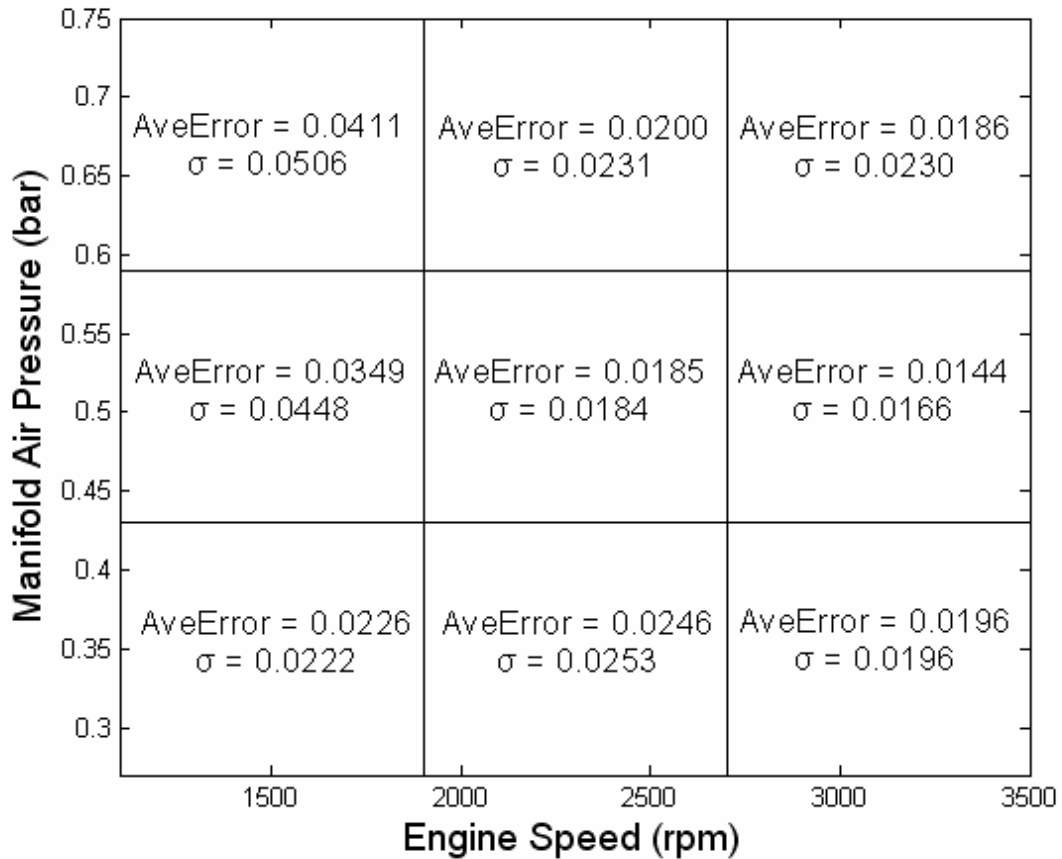


Figure 31: Error Statistics of Mass Fraction Burned Prediction by Region

Chapter 5: Results

After the combustion model was validated, it was implemented into GT-Power. The other sections of the model had already been composed so the complete engine model was ready to be tested. Although the accuracies of the individual components of the model were proven, the complete model was not guaranteed to be representative of the engine. Therefore several hundred operating conditions were chosen and simulated using the GT-Power model. These results were compared with the experimental data and had a high correlation. The final model did require some modification to increase its accuracy. However, the combustion model remained unchanged.

Although the model was validated it still had some limitations. Because the combustion coefficients were found using a step-wise regression, their equations are only valid over a specific range. The model was created using only a small number of data points and the data only spanned part of the target range. Inside the range encompassed by the experimental data, the model produced very accurate results. Too far outside the experimental data range, the model was unpredictable. The experimental data anchors the regressions. Outside of the range of the experimental data, the regression could produce unrealistic or unphysical results. To ensure that the output of the regressions is not outrageous, each output was bounded. The range for each coefficient was determined from the experimental data.

5.1 GT-Power's Crank Angle Resolved Capabilities

GT-Power is able to provide a great deal of information about the engine once it has been calibrated. All of GT-Power's outputs are steady-state values. To demonstrate

the capabilities of GT-Power, a typical operating point was examined and the results are provided. The operating condition was an engine speed of 1500 rpms and an intake manifold pressure of 30 kPa. One of the targets of the GT-Power model using in this research is to determine the effect of manipulating the cam angles. The exhaust and intake cam profiles as well as the velocity of the valves over one engine cycle is shown in Figures 32 and 33. Through comparisons of different cam profiles and timing, GT-Power can be used to pick the optimum cam shafts.

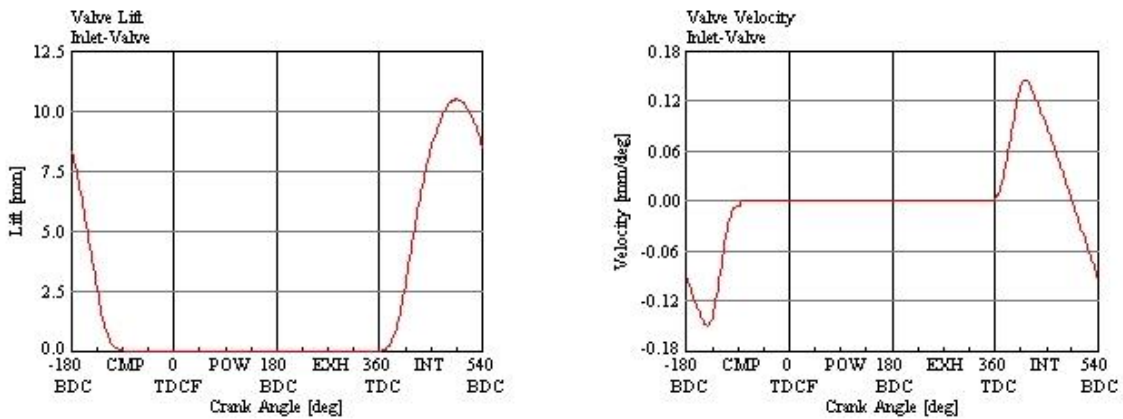


Figure 32: Intake Valve Lift and Velocity (1500 rpm, 0.3 bar)

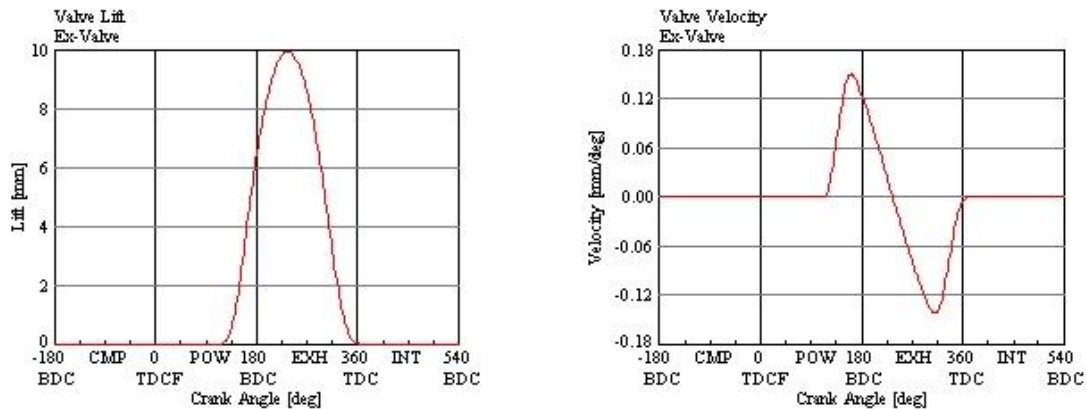


Figure 33: Exhaust Valve Lift and Velocity (1500 rpm, 0.3 bar)

GT-Power can also be used to determine several parameters relative to the intake. Tuning the wave dynamics of an intake system is important for producing maximum

power. For maximum power, a wave should reach the intake ports right as the intake valves close. The wave dynamics of the intake system are shown Figure 34. It is important to notice that wave dynamics have a significant impact on the pressure of the intake. The amplitude of the wave is about 2 percent of the average pressure and the oscillations are at a very high frequency. High frequency oscillations can create aliasing in experimental data. To prevent aliasing, a high order low pass filter was used to attenuate the high frequency waves.

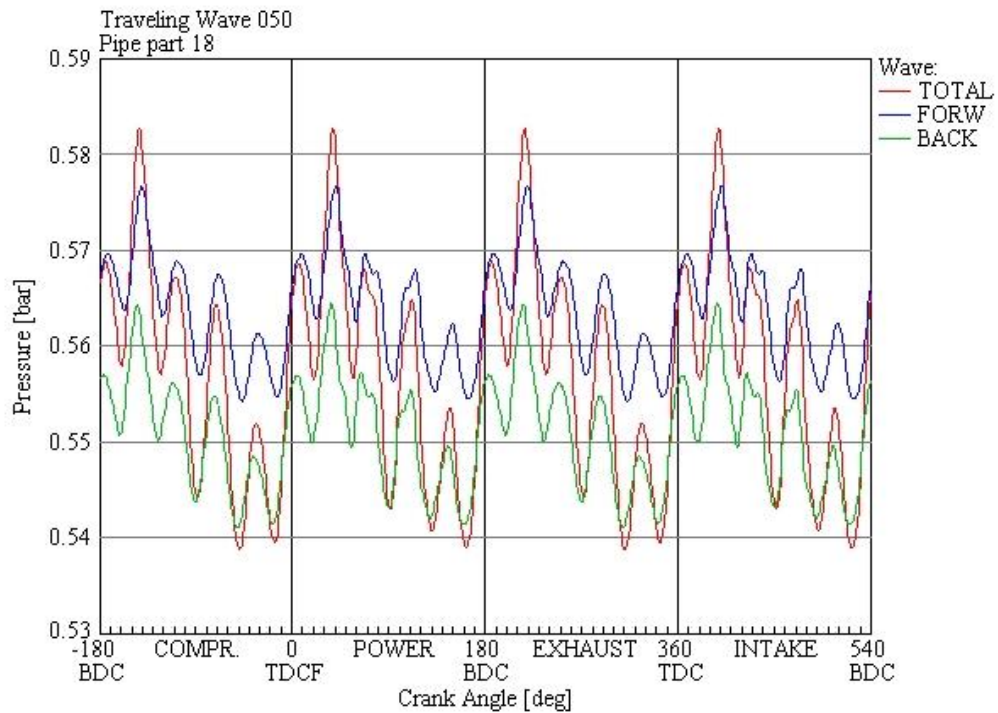


Figure 34: Wave Dynamics of the Intake System (1500 rpm, 0.3 bar)

Each component in the intake system can provide information about the wave dynamics, the wall temperature, the charge temperature, the pressure and the flow rates. The wall temperature of the one of the intake runners is shown in Figure 35. A combination of the wall temperature and/or charge temperature can be used for controlling on an engine. Although oxygen sensors in the exhaust system are used as

feedback for the air/fuel ratio control, the majority of the control is based on air charge temperature and a mass air flow sensor. The volumetric efficiency of an engine is often used to predict the air entering an engine. By knowing the volumetric efficiency at an operating point and the charge temperature, the trapped mass of air can be calculated.

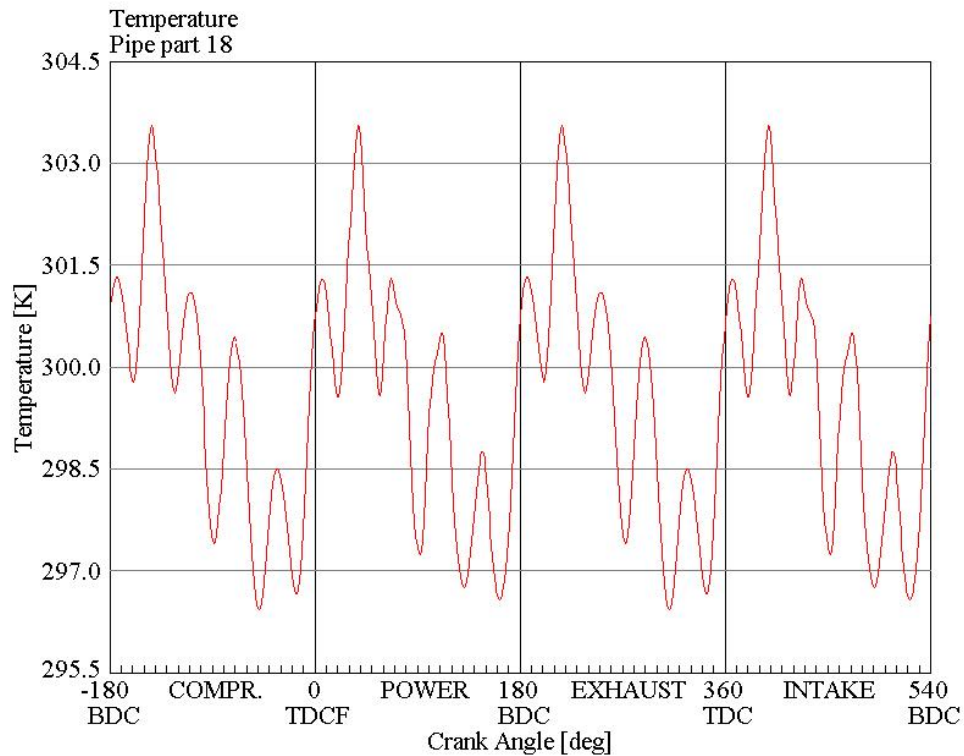


Figure 35: Wall Temperature of the Intake System (1500 rpm, 0.3 bar)

Therefore choosing the location of these sensors on an engine is important. Ideally the actual charge temperature would be measured, but this is difficult to implement. Normally the air charge sensor is placed in the intake runners just before the engine head. GT-Power can be used to determine the best spot to put a wall or charge temperature sensor. The actual air charge temperature is mostly dependent upon the heat transfer from the intake walls. Figure 36 shows the heat transfer from the intake walls to the air. GT-Power can facilitate the creation of an air charge temperature prediction

model. It can also be used to calculate the volumetric efficiency. This will be discussed later in the paper.

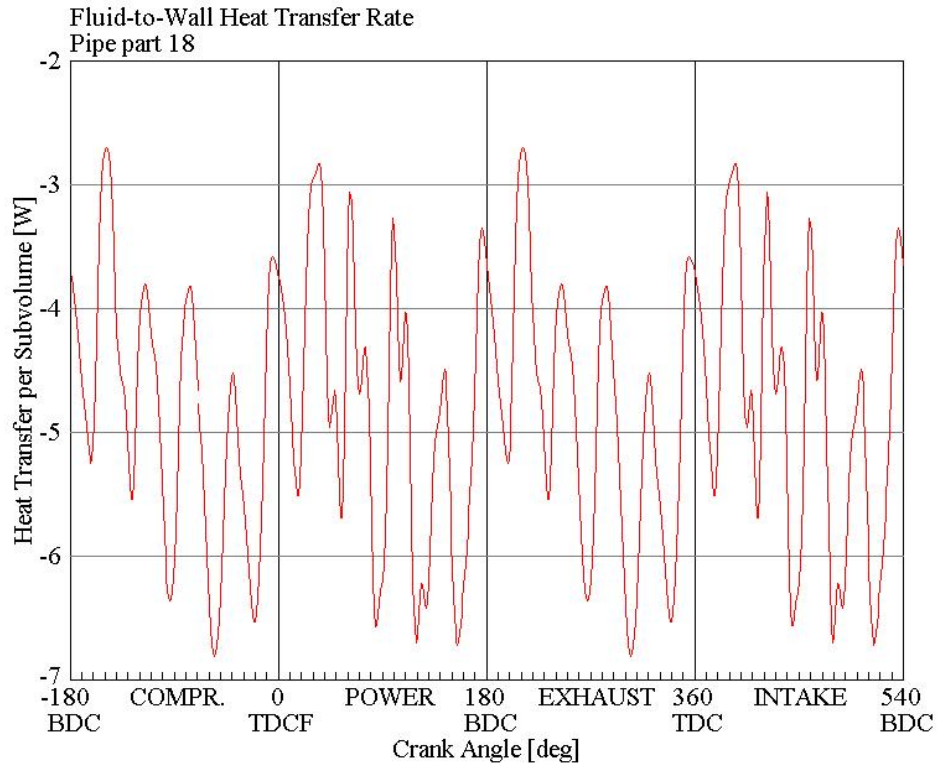


Figure 36: Charge Temperature of the Intake System (1500 rpm, 0.3 bar)

Another measurement using feedback control is mass air flow. Figure 37 shows the mass flow rate of air through the throttle. To control the load on an engine, the throttle angle is adjusted to restrict the mass flow rate of air. GT-Power can also be used to predict the pressure drop across the throttle as shown in Figure 38. Cam phasing can reduce the need to throttle and can therefore reduce the flow losses related to throttling. At this moderate load condition, the pressure is cut nearly in half. Obviously the fluid losses across the throttle are significant. In terms of engine control, the throttle angle is difficult to measure accurately since it vibrates. Therefore, the intake manifold pressure is used. The intake manifold pressure is the difference between the ambient pressure and

all of the pressure drops due to fluid friction. The manifold pressure is shown in Figure 39. The pressure losses due to fluid friction from everything except the throttle are negligible.

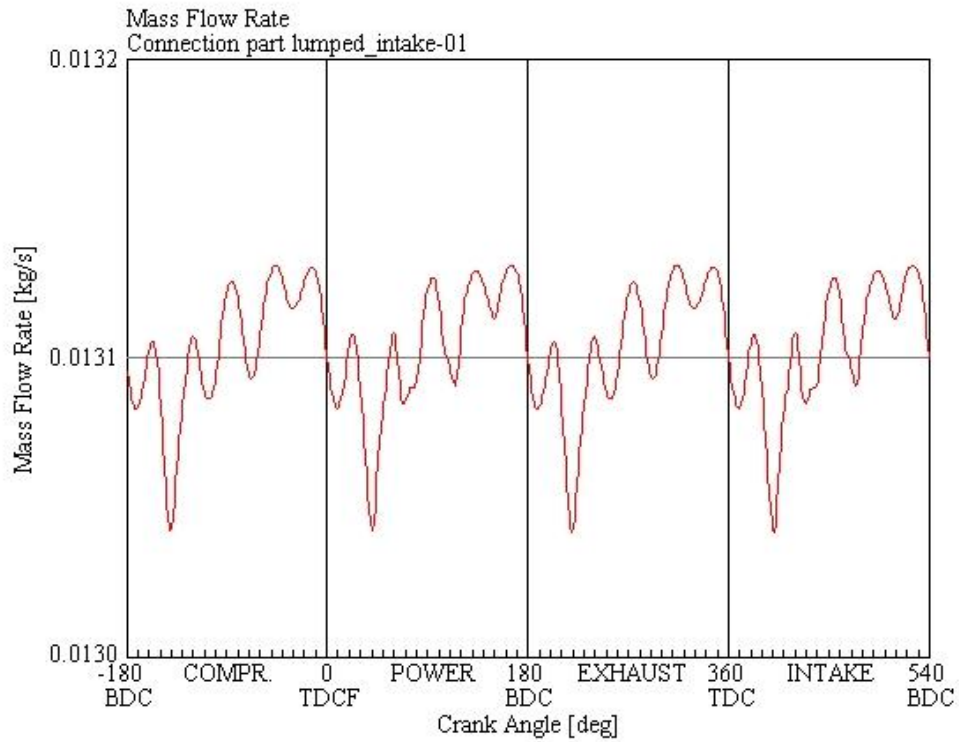


Figure 37: Mass Flow of Air through the Throttle (1500 rpm, 0.3 bar)

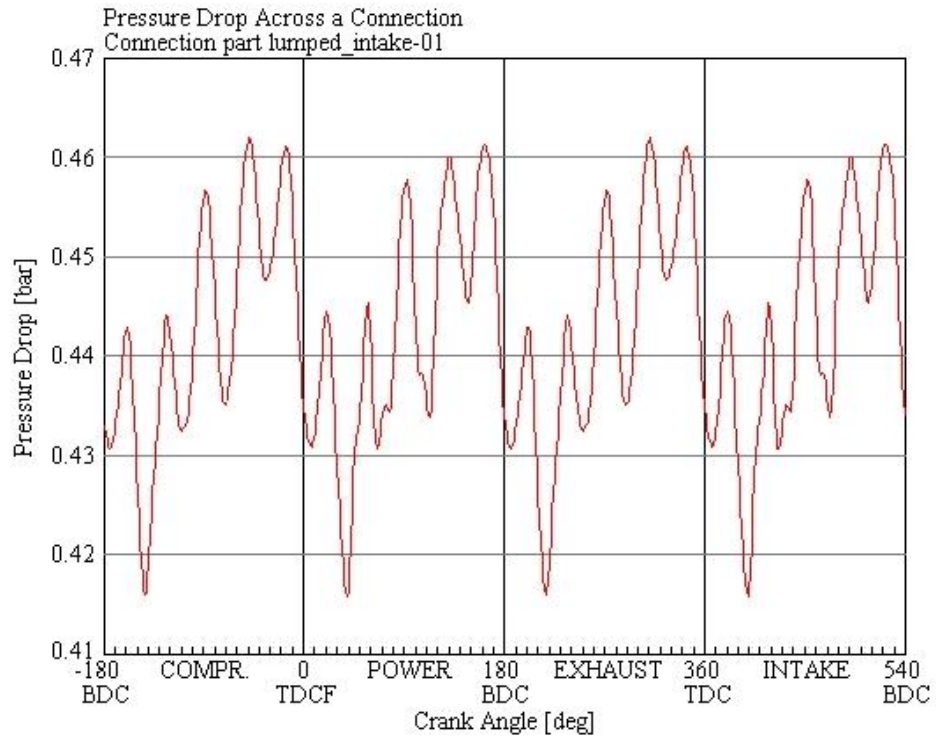


Figure 38: Pressure Drop across the Throttle (1500 rpm, 0.3 bar)

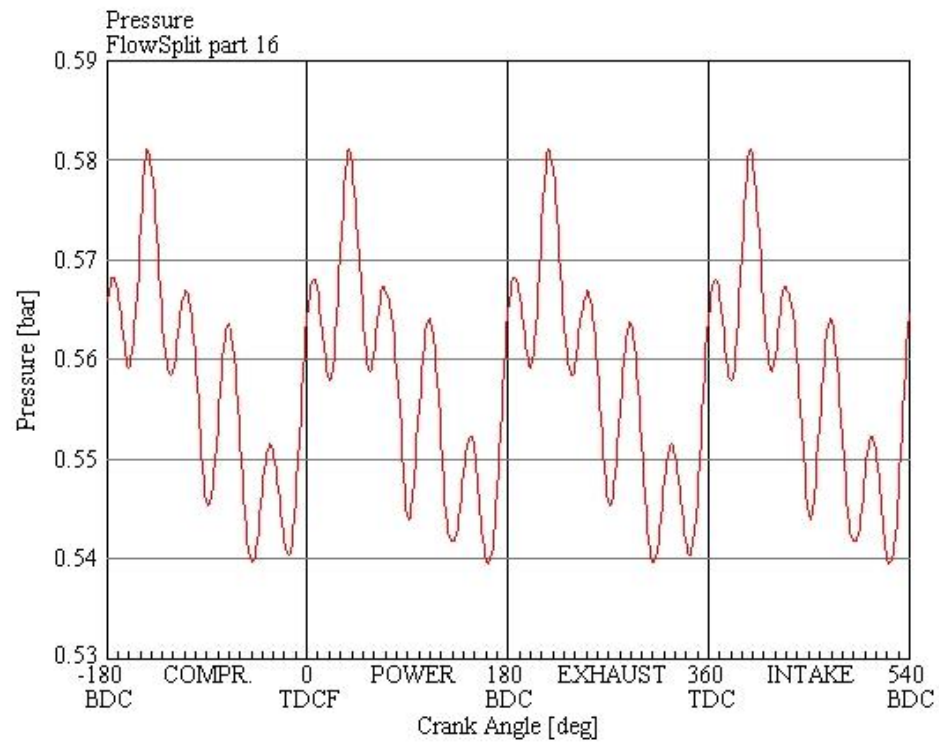


Figure 39: Manifold Air Pressure (1500 rpm, 0.3 bar)

Another major strength of GT-Power is the ability to see the output parameters related to combustion. The fuel delivery rate is shown in Figure 40. Selection of a fuel injector is largely based on its maximum fuel delivery rate. Therefore, a fuel injector can be chosen based on the required fuel delivery rate generated by GT-Power. From the combustion model that was used to calibrate GT-Power the in-cylinder pressure is generated. Figure 41 shows the pressure rise over one engine cycle. In this form, engine knock can easily be detected and so can the peak pressure. When engine knock is present, the increasing edge of the pressure trace will be jagged instead of smooth. Another important quantity that can be extracted from this graph is the indicated mean effective pressure (IMEP). This is a measure of the torque before any mechanical losses of the transmission. Alternately, if the pressure is graphed against the cylinder volume the net and pumping work can be determined. The net work is the upper loop and the pumping work is the lower loop as shown in Figure 42. It is possible to nearly completely eliminate the pumping work by adjust the cam timing.

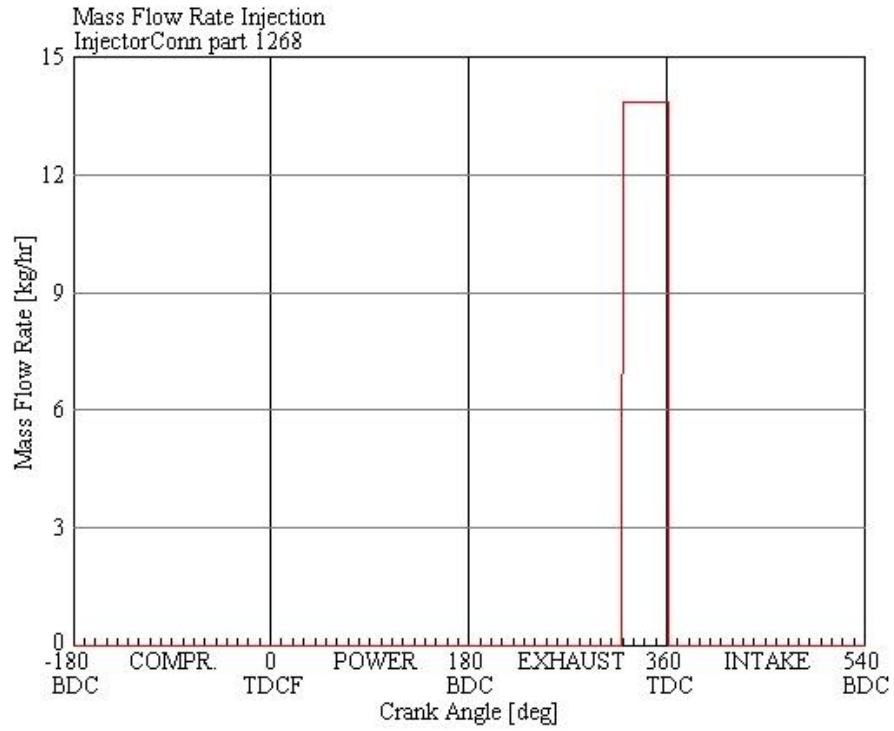


Figure 40: Mass Flow of Injected Fuel (1500 rpm, 0.3 bar)

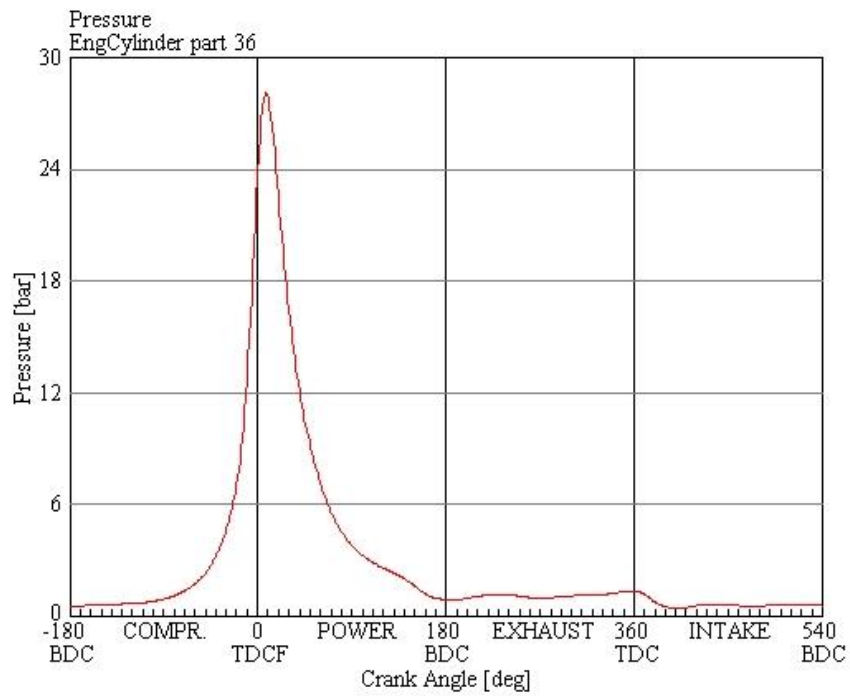


Figure 41: In-cylinder Pressure (1500 rpm, 0.3 bar)

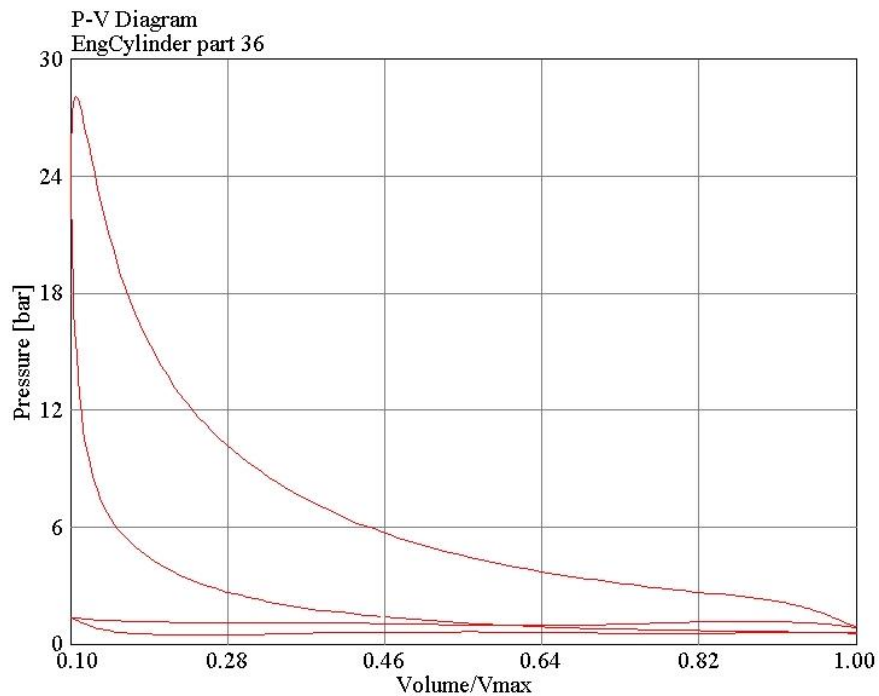


Figure 42: Pressure-Volume Diagram (1500 rpm, 0.3 bar)

GT-Power can also provide several other burn rate illustrations. All of the combustion outputs are based on the combustion model. The mass fraction burned curve generated from the combustion model is presented in Figure 43. As expected the curve has two modes of combustion. From this curve the apparent heat release rate is calculated as shown in Figure 44. These parameters are calculated for each cylinder and then they are combined to find the torque output. The overall torque output of the engine is graphed in Figure 45.

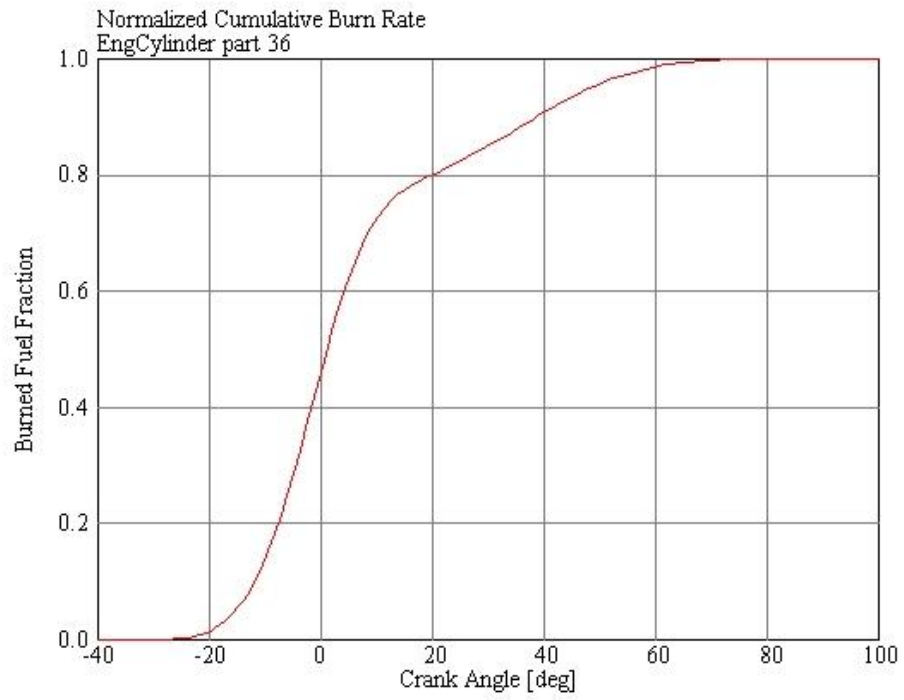


Figure 43: Normalized Cumulative Burn Rate (1500 rpm, 0.3 bar)

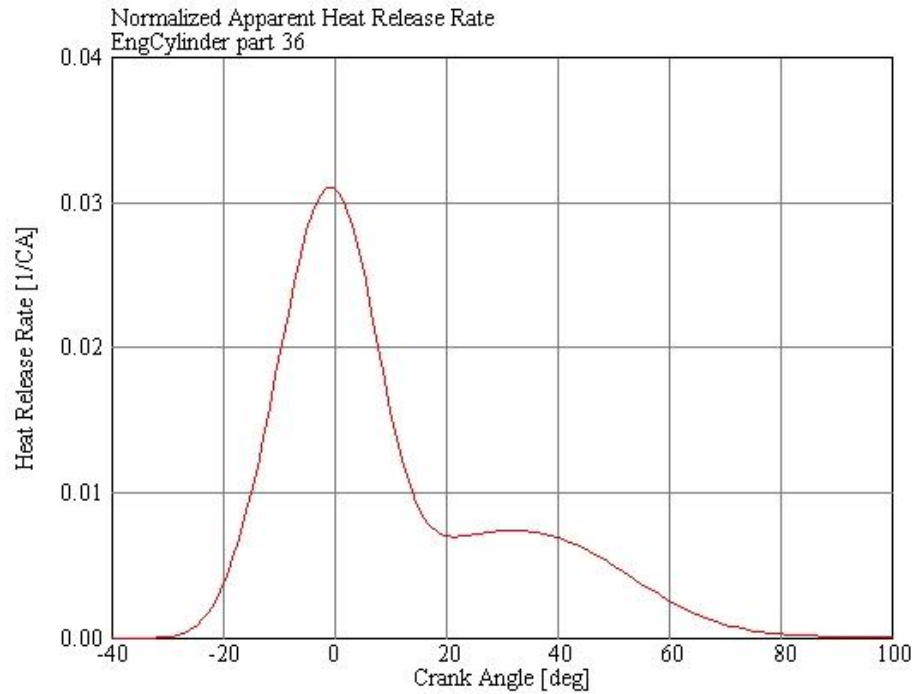


Figure 44: Normalized Apparent Heat Release Rate (1500 rpm, 0.3 bar)

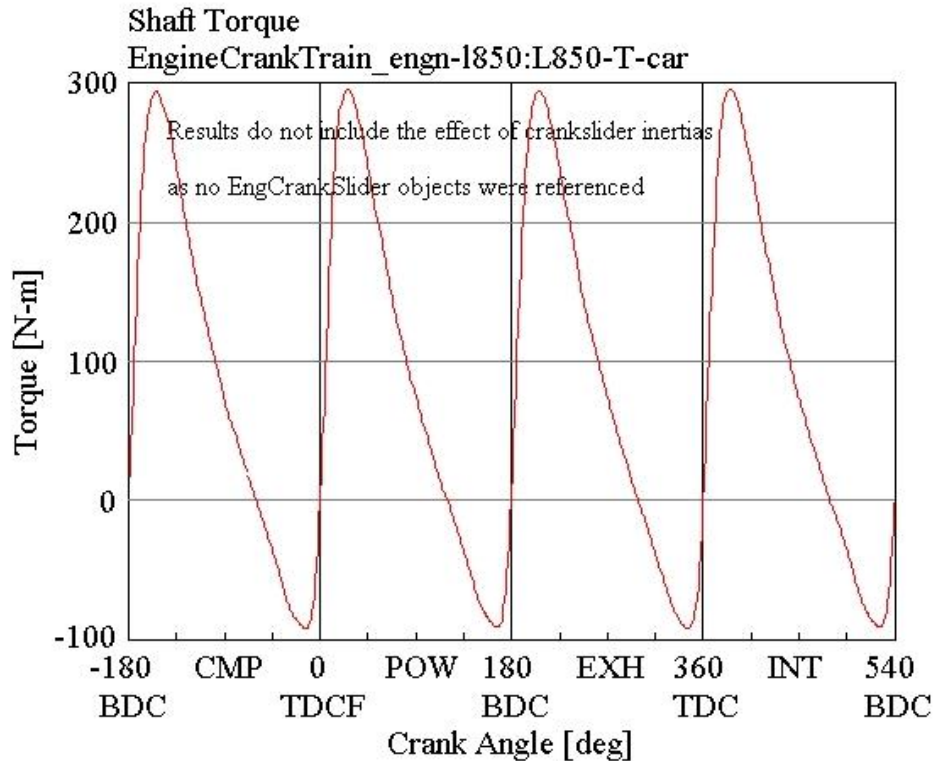


Figure 45: Overall Output Torque (1500 rpm, 0.3 bar)

5.2 GT-Power Cycle Average Capabilities

Although the crank angle resolved data provided by GT-Power is extensive and powerful, the cycle average data is more often used. For most parameters it is easier to compare operating points based on a single value rather than analyzing raw cycle data. To illustrate the effect of the cam timing, a group of operating points will be examined. The engine speed and manifold pressure are held constant with the intake and exhaust cams swept through every possible combination. The operating point that was chosen is one of the most commonly encountered in normal driving. The engine speed and manifold air pressure were set to 2000 rpm and 0.49 bar. In the government mandated FTP drive cycle, which represents city driving, this operating point is right in the middle as shown in Figure 46.

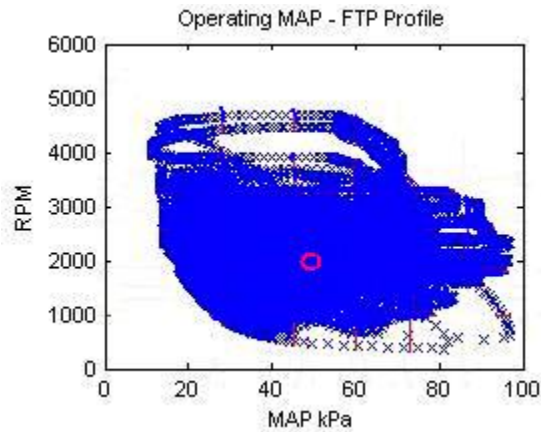


Figure 46: Operating Points Encountered during a FTP Cycle (2000 rpm, 0.49 bar)

In-cylinder pressure traces provide a wealth of information but are often reduced to a single characteristic, namely, indicated mean effective pressure (IMEP). IMEP is the average pressure over one engine cycle. IMEP is an indirect measure of the torque output and combines the effects of the peak pressure and pumping work. The effect of cam timing on IMEP is shown in Figure 47.

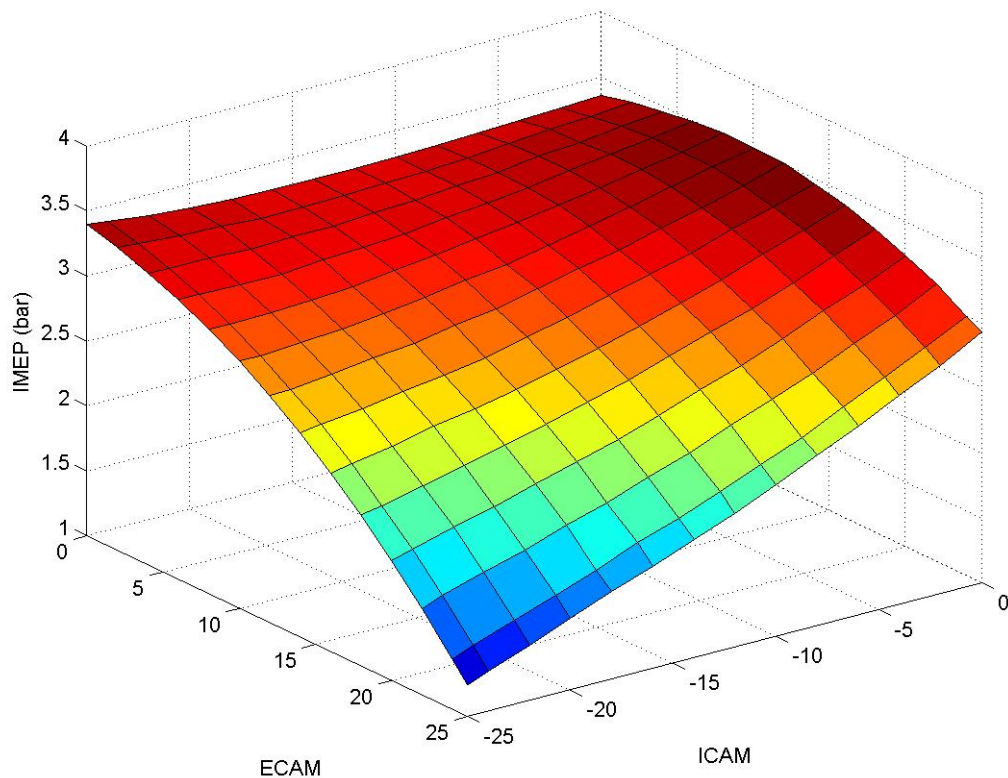


Figure 47: Effect of Cam Timing on IMEP (2000 rpm, 0.49 bar)

The surface that is generated by sweeping the intake and exhaust cams shows several pairs of cam angles that produce reasonable IMEP. When the exhaust cam is retarded 25 degrees and the intake is advanced 25 degrees, the IMEP drops off dramatically. This is an indication that the combustion is very poor. When the exhaust cam is retarded and the intake is advanced, the valve-overlap increases. The low IMEP produced at a fully retarded exhaust cam and fully advanced intake cam is a result of the extreme valve-overlap. Excluding conditions with large valve-overlap, the IMEP is around 3.3 bar. Because several cam positions produce nearly the same IMEP, other parameters can be considered when choosing the optimum cam positions. The maximum

IMEP of 3.5 bar occurs with an exhaust cam position of 10 degrees and an intake cam position of 0 degrees, the parked position.

One of the largest determining factors of the IMEP is the amount of air trapped per engine cycle. Engines are run as close to a stoichiometric fuel ratio as possible. Therefore, the air trapped per engine cycle is proportional to the amount of fuel injected. Assuming all of the fuel is burned, increasing the fuel injected also increases the peak pressure and the IMEP. The surface generated by graphing the trapped air versus the cam positions as seen in Figure 48 is very similar to the IMEP graph. When the intake and exhaust cams are both shifted 25 degrees, the trapped air is at a minimum. The maximum amount of trapped air occurs when the intake cam is parked and the exhaust cam is shifted 10 degrees. Both the maximum and minimum trapped air masses occur at the same conditions that produce the maximum and minimum IMEP.

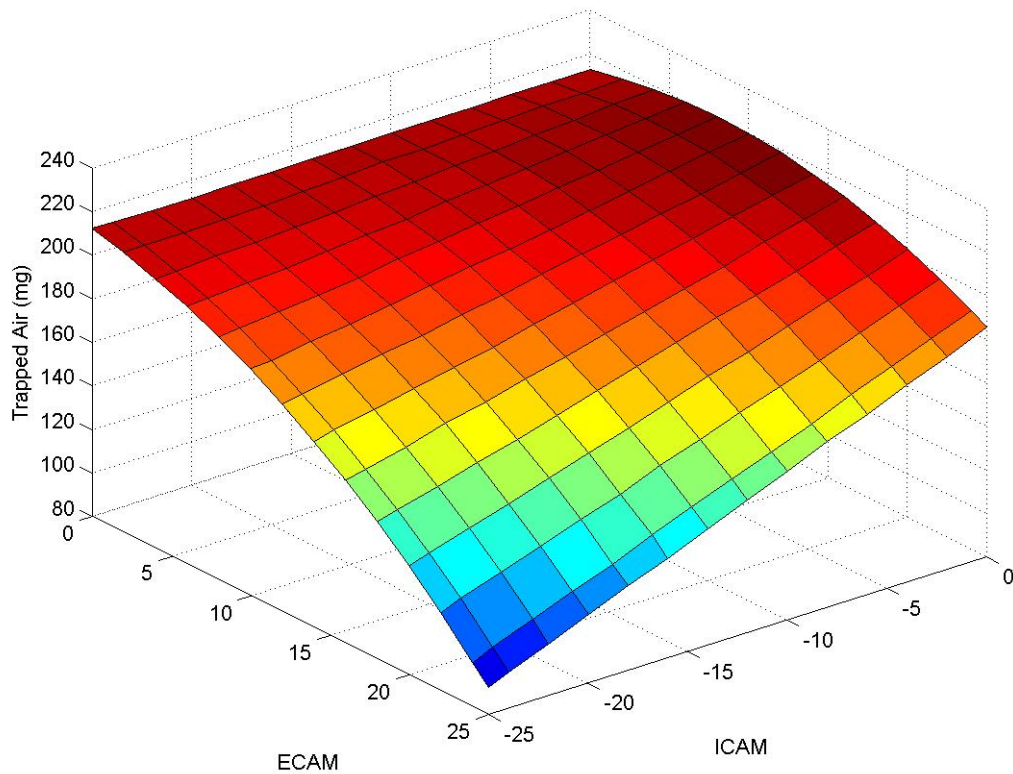


Figure 48: Effect of Cam Timing on Trapped Air Mass (2000 rpm, 0.49 bar)

Although it appears that condition induces the most air and produces most torque is the optimum condition. Excluding conditions with very high valve overlap, the IMEP and trapped air mass surfaces are flat. To distinguish these points on a seemingly flat surface, the indicated fuel conversion efficiency can be introduced. Indicated fuel efficiency is a measure of how well an engine convert the stored energy of fuel into useful mechanical work. Equation 12 show the relationship between trapped mass, IMEP and indicated fuel conversion efficiency.

$$\eta_{f,i} = \frac{V_d IMEP}{m_f Q_{LHV}}$$

Equation 12: Indicated Fuel Conversion Efficiency

In all of the simulations the air/fuel ratio was stoichiometric, so the mass of fuel is equivalent to the mass of air divided by 14.6. Using this relationship and Equation 12, the indicated fuel conversion efficiency was calculated as a function of cam timing. As seen in Figure 49, the fuel conversion efficiency curve is not nearly as flat as either the IMEP or trapped mass curves. The most efficient condition occurs when the intake cam is parked and the exhaust is retarded 15 degrees. However when the intake is advanced 25 degrees and the exhaust cam is parked, the efficiency is nearly as high. This graph also shows the dramatic effect cam phasing has on fuel efficiency. From the most efficient to the least efficient cam pairs, the efficiency changes over 5 percent.

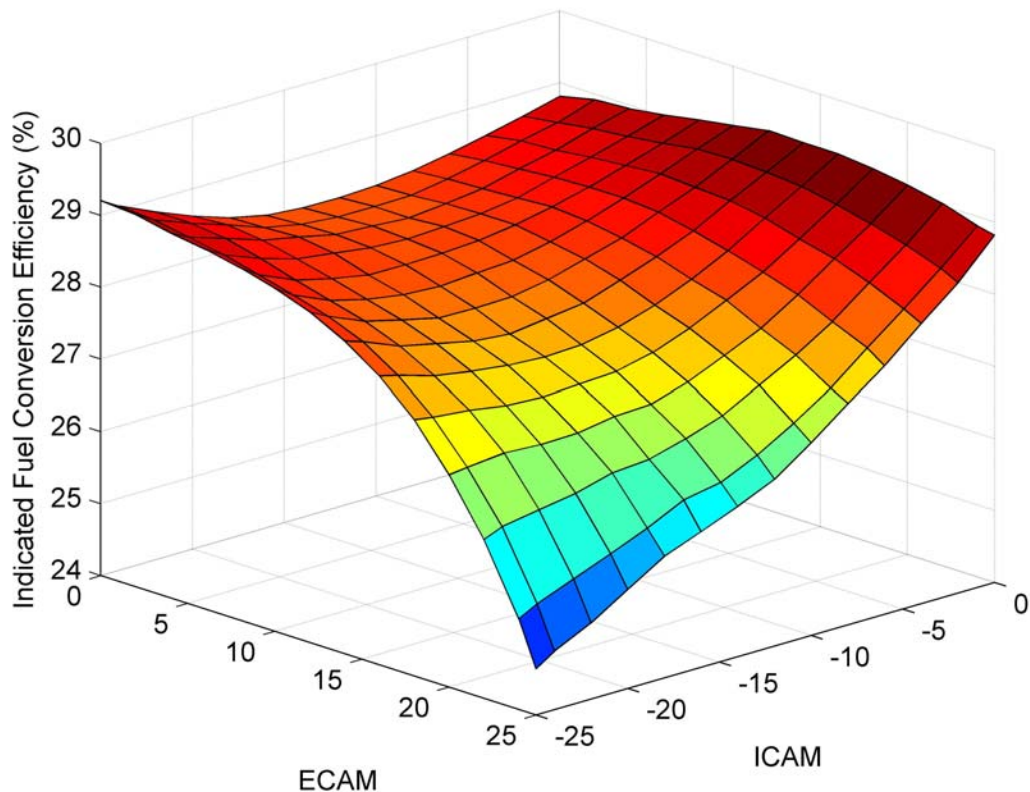


Figure 49: Effect of Cam Timing on Indicated Fuel Conversion Efficiency (2000 rpm, 0.49 bar)

As previously described, one of the largest causes of the minimum in the trapped air and IMEP is the valve-overlap. A large amount of valve-overlap causes an increase in the trapped residual gases. When the exhaust timing is retarded and the intake timing is advanced, there is a portion of time where both the intake and exhaust valves are open. This condition is called valve-overlap. The pressure inside the intake manifold is considerably lower than the exhaust manifold. So when both the intake and exhaust valves are open, the pressure gradient causes the combustion gasses to flow from the exhaust system into the intake. Once the exhaust valves close and the pressure inside the combustion chamber reduces, the flow changes directions again. The result is a combination of combustion gases and fresh air charge is pulled back into the engine's cylinders. Figure 50 shows the effect of cam timing on the trapped residual gas mass.

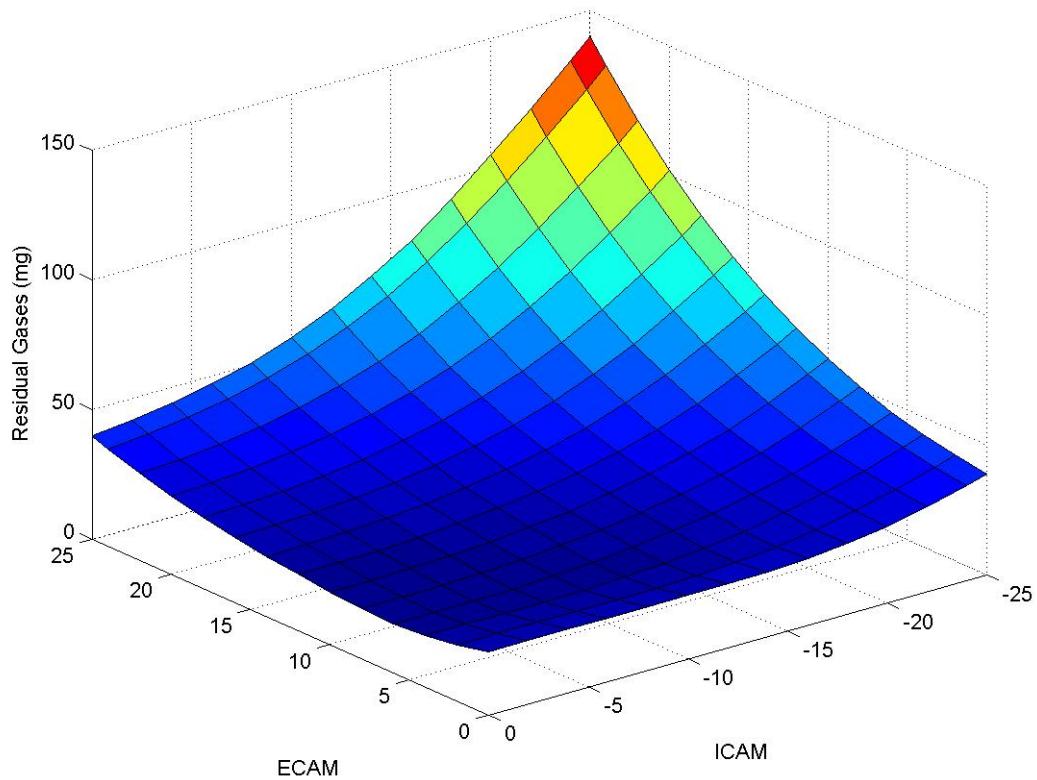


Figure 50: Effect of Cam Timing on Trapped Residual Gases (2000 rpm, 0.49 bar)

Residual gases are composed mostly of carbon dioxide, nitrogen and possibly nitrogen oxides. Unless the previous cycle was a misfire, the residual gases will not contain fuel. Similarly unless the previous cycle was run at a very lean air/fuel ratio, the residual gases will contain neglectable amounts of oxygen. Residual gases will therefore not burn. For this reason it is important to consider the percentage residual gases induced. Figure 51 shows the mass percentage of residual gases as a function of cam timing. Compared to condition around parked where the valve overlap is small or zero, the highest valve overlap condition has a dramatically higher percentage residual gases. At the maximum valve overlap condition the residual gases comprise 60 percent of the gases in the combustion chamber. Unless there is adequate mixing, the local concentration

around the spark plug could be almost all residuals. If this happens, then no combustion will propagate causing a misfire.

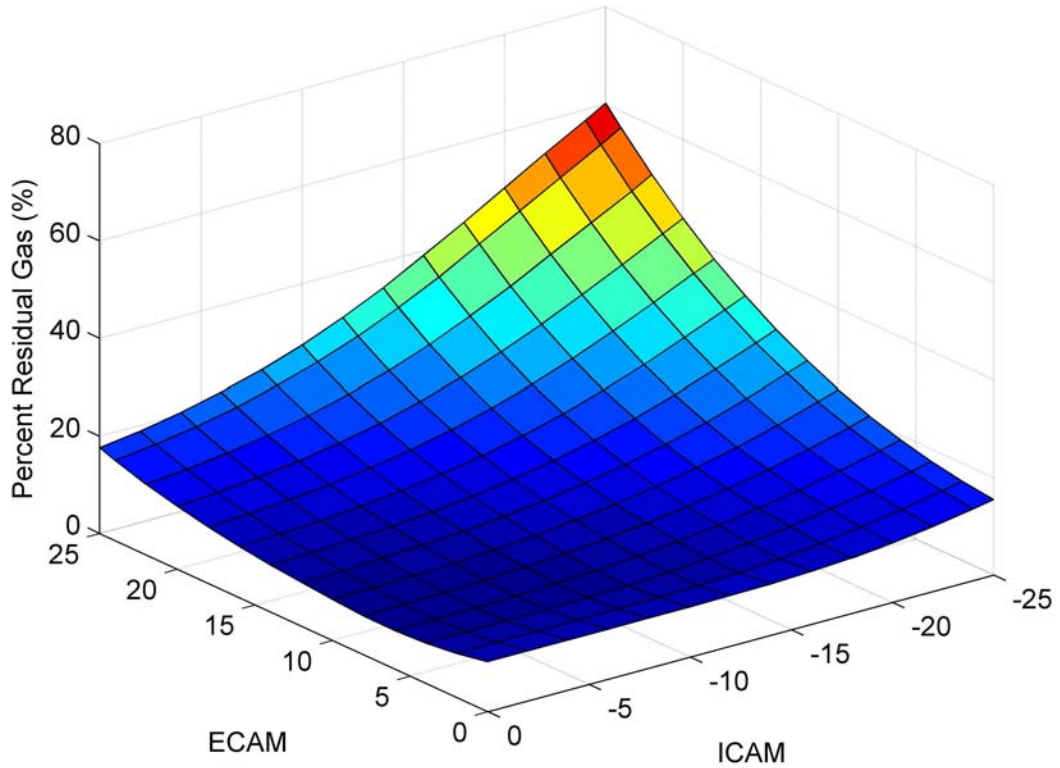


Figure 51: Effect of Cam Timing on Residual Gas Fraction (2000 rpm, 0.49 bar)

As expected the highest mass of trapped residuals occurs when the exhaust cam is fully retarded and the intake cam is fully advanced. In general, an increase in valve-overlap increases the amount of trapped residuals. It is also important to notice that even when both the intake and exhaust cams are parked some residuals are still present. At the park condition the valve-overlap is zero, but not all of the exhaust gases are forced out. Because engine cylinders have a clearance or minimum volume, a portion of the exhaust gases will always remain after the exhaust valves close.

Residual gases have several effects both beneficial and detrimental. The largest use of residual gases is to reduce the temperature of combustion. During normal operation conditions a small amount of residual gases is desired to dilute the air mixture and thus reducing the temperature of combustion. A lower peak combustion temperature reduces the formation of nitrous oxides. On the downside, too much valve-overlap can prevent air from being inducted. A concentration of residual gases too high can inhibit normal combustion. This is why the IMEP was so low when both cams were shifted 25 degrees.

Residual gases have another impact on engines. Because hot combustion gases are being mixed with cool ambient air, the temperature of air is increased. The mass of both the air and residual gases is so small that the temperature change is nearly instantaneous. The air charge temperature is shown in Figure 52 as a function of the cam positions. Having a higher charge temperature affects the thermal efficiency and the volumetric efficiency. Assuming air is an ideal gas, a higher temperature increases the volume of the gas. Because the volume displaced by an engine is fixed, the mass of air that can be captured is reduced. ECUs often use air charge temperature in predicting the trapped air mass.

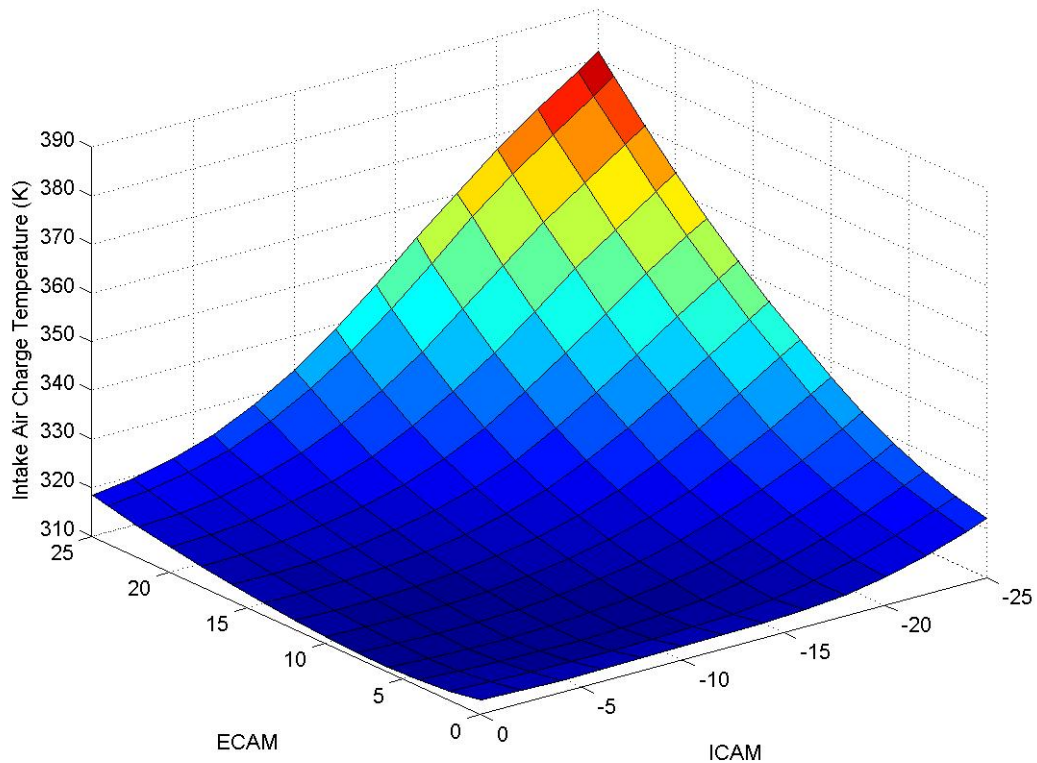


Figure 52: Effect of Cam Timing on Air Charge Temperature (2000 rpm, 0.49 bar)

The volumetric efficiency is a measure of the ability of an engine to induct air into its cylinders. Maximizing the volumetric efficiency is always a high priority. As seen from the graph in Figure 53, the volumetric efficiency is relatively constant for a majority of the cam pairs. At very high valve overlap conditions, the concentration of residual gases is very high. The pressure of the residual gases is nearly atmospheric which is about double the pressure of the intake air. Because the residuals are at such a high pressure initially, they occupy a large volume when they reach an equilibrium pressure equal to the manifold pressure. Most of the gas that is induced is residual gas and not air. The charge temperature is also larger than normal when the overlap is large.

Therefore the density of the gas is decreased. Compared to the parked condition the mass of the trapped air is smaller at the same volumetric efficiency.

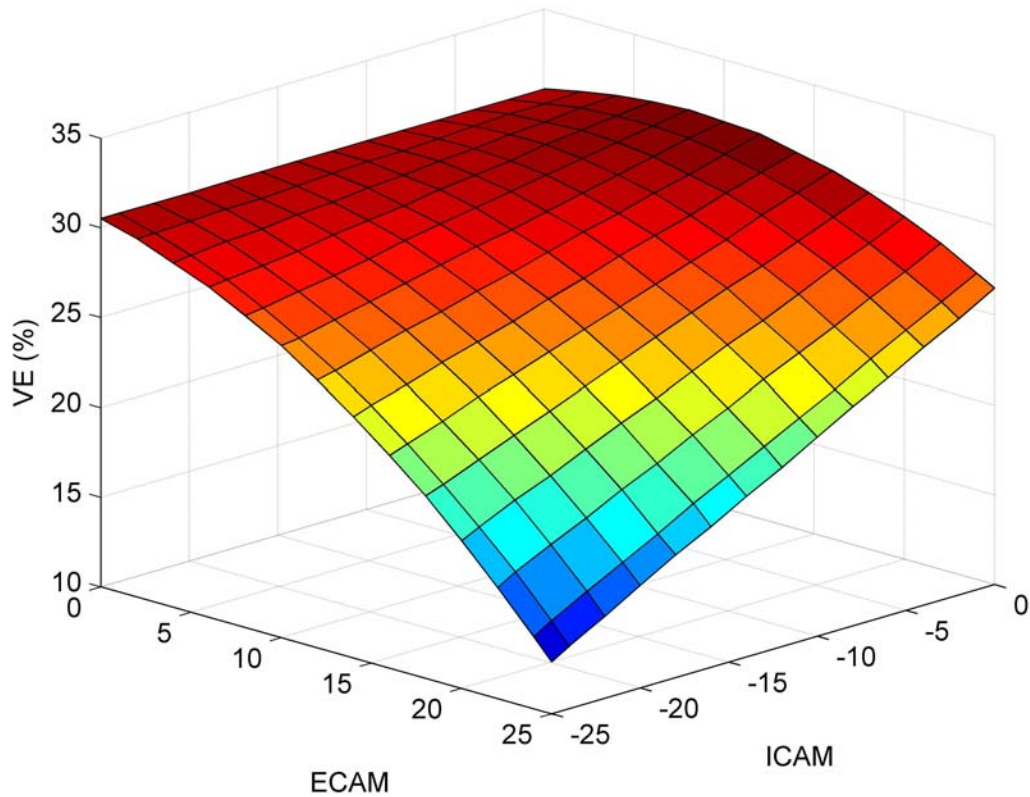


Figure 53: Effect of Cam Timing on Volumetric Efficiency (2000 rpm, 0.49 bar)

To find the volumetric efficiency, the actual amount of air inducted is divided by the maximum possible volume of air which is equal to the engine's displacement. This relationship is shown in Equation 13.

$$\eta_v = \frac{m_a}{\rho_{a,i} V_d}$$

Equation 13: Volumetric Efficiency

In many vehicles the volumetric efficiency is stored in a table as function of the operating conditions (engine speed, manifold air pressure, intake cam positions and exhaust cam position). Using some form of interpolation, the ECU determines the volumetric efficiency. Then by measuring the air temperature at the intake valve inlet, the ECU calculates a predicted trapped air mass. This air mass is then used in conjunction with exhaust gas oxygen sensors to control the air/fuel ratio.

Another measure of the engine's efficiency is the manifold volumetric efficiency. Unlike the normal volumetric efficiency which uses the density of air entering the engine, the manifold volumetric efficiency uses the density of the air in the manifold. The manifold volumetric efficiency as a function of cam timing is shown in Figure 54. The maximum efficiency is at an exhaust position of 4 and an intake position of 15

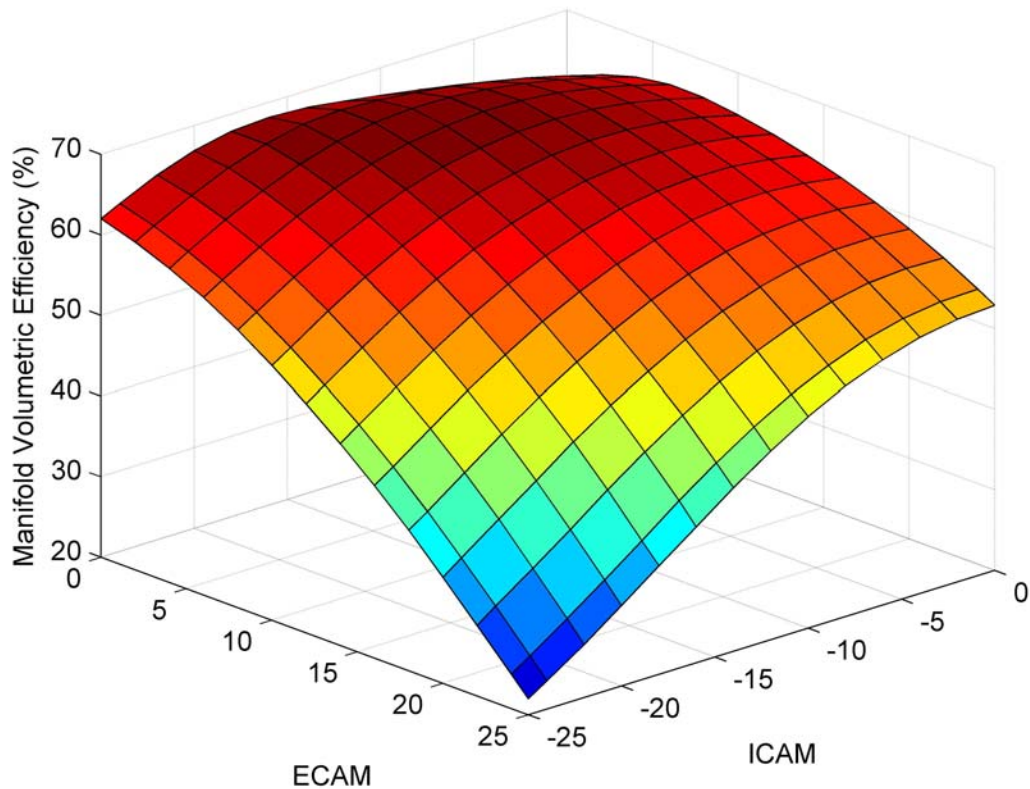


Figure 54: Effect of Cam Timing on Manifold Volumetric Efficiency (2000 rpm, 0.49 bar)

Above all of the previous parameters, combustion stability must always be considered. If the combustion is erratic or produces knock, then that combination of conditions would be avoided at all costs. It is very important to identify all possible cam pairs that produce unstable and potentially dangerous combustion. Although cam pairs that produce knock would never be input, they might occur during a transient. Consider an engine operating at a high engine speed and moderate load where high overlap is common. Now assume that the driver performs a hard tip-out (deceleration). The new target cam positions would move away from the high overlap conditions. However because cam phasers have a finite response time, the engine may briefly encounter

conditions that produce engine knock. By knowing that knock is possible, a control strategy could proactively prevent it by retarding the spark timing.

Two major factors indicate undesirable combustion. These factors are combustion duration and the crank angle at the start of combustion. Figure 55 shows the variation in the combustion duration as a function of the intake and exhaust positions. Quality combustion cannot happen too fast or too slow. Combustion that occurs extremely rapidly can be dangerous. Normal combustion has a physical lower bound that is limited by the flame speed. If the combustion duration is very short, then multiple flame fronts must have been generated. The secondary flame fronts can be caused from auto-ignition and can destroy an engine.

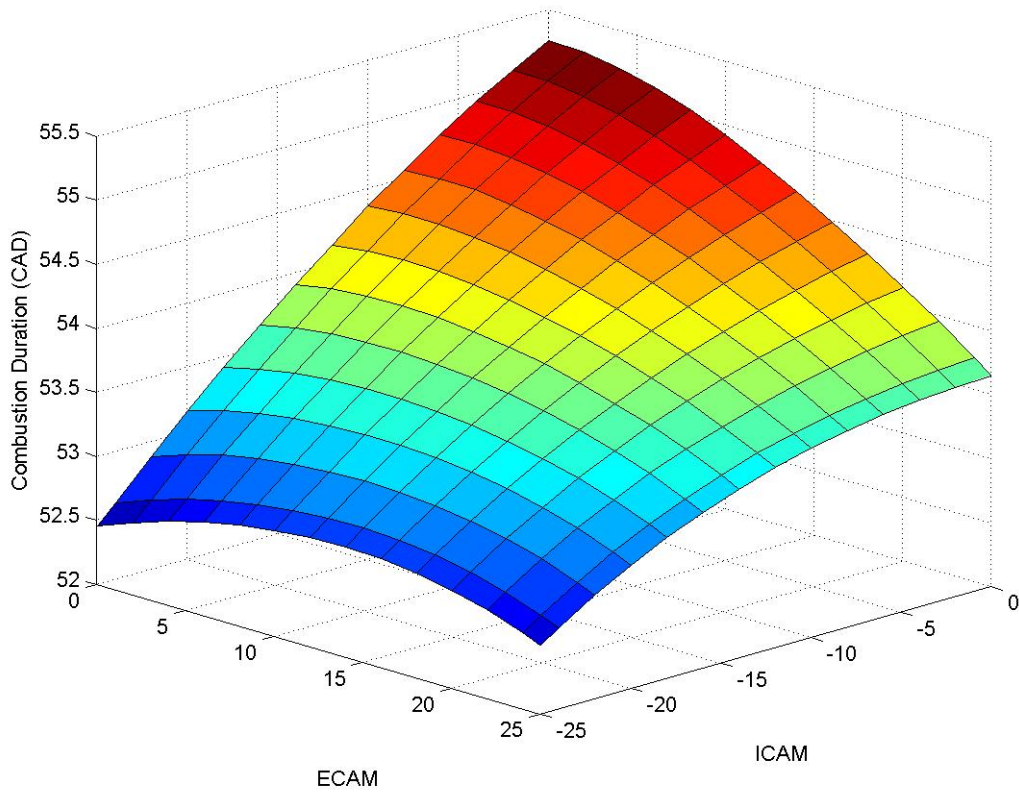


Figure 55: Effect of Cam Timing on the Combustion Duration (2000 rpm, 0.49 bar)

The upper bound on the combustion limit is a practical limit. The travel of a piston changes the pressure and volume of the combustion chamber. An engine makes power by exerting a force on the piston face. There is a window of crank angles where combustion is effective. If combustion occurs outside this region, then the pressure increase due to the combustion is reduced. Therefore slow combustion has most of the pressure increase occurring outside the optimum region. For the same reasons, the start of combustion is very important. If combustion occurs too early, then the peak pressure could occur before the piston reaches top dead center. When this happens, the combustion is opposing the motion of the piston instead of generating power. The variation in the start of combustion due to the cam timing is shown in Figure 56. Spark timing has a significant impact on the start of combustion. Therefore spark timing could be used to counteract the effect of cam timing on the start of combustion.

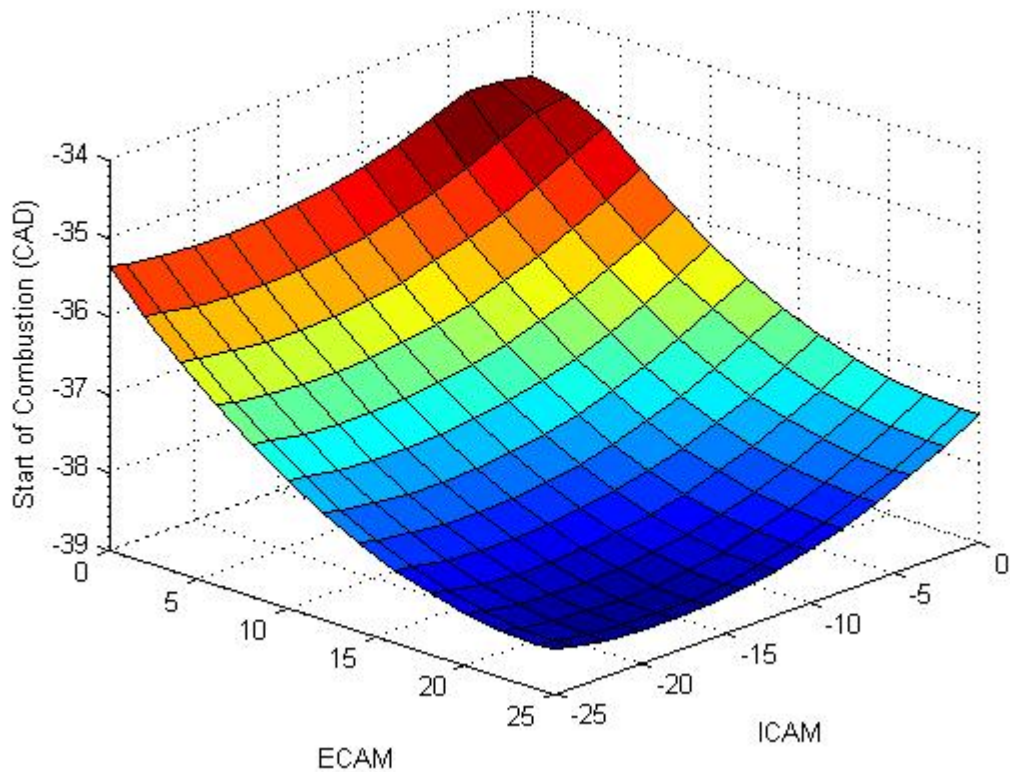


Figure 56: Effect of Cam Timing on the Start of Combustion (2000 rpm, 0.49 bar)

The two previous figures show the effect of cam timing on combustion duration and the start of combustion. These differences do not do the variation in combustion justice. To better illustrate the variation in combustion, the in-cylinder pressure traces of a few extreme cam pairs are shown in Figure 57. The five cases shown are the four corners of the possible cam pairs and the center cam pair. The lowest peak pressure, 17 bar, occurred when the cams were parked. On the other hand, the highest peak pressure, 27 bar, occurred when the intake is parked and the exhaust cam is retarded 25 degrees. The other cam pairs produce peak pressures that fall within this range. Another difference between cam pairs is the drop in pressure during the intake stroke. The pressure during the intake stroke (360 – 540 degrees) is lower than atmospheric and

therefore requires work. The best cam would have a high peak pressure and a near atmospheric pressure during the intake stroke.

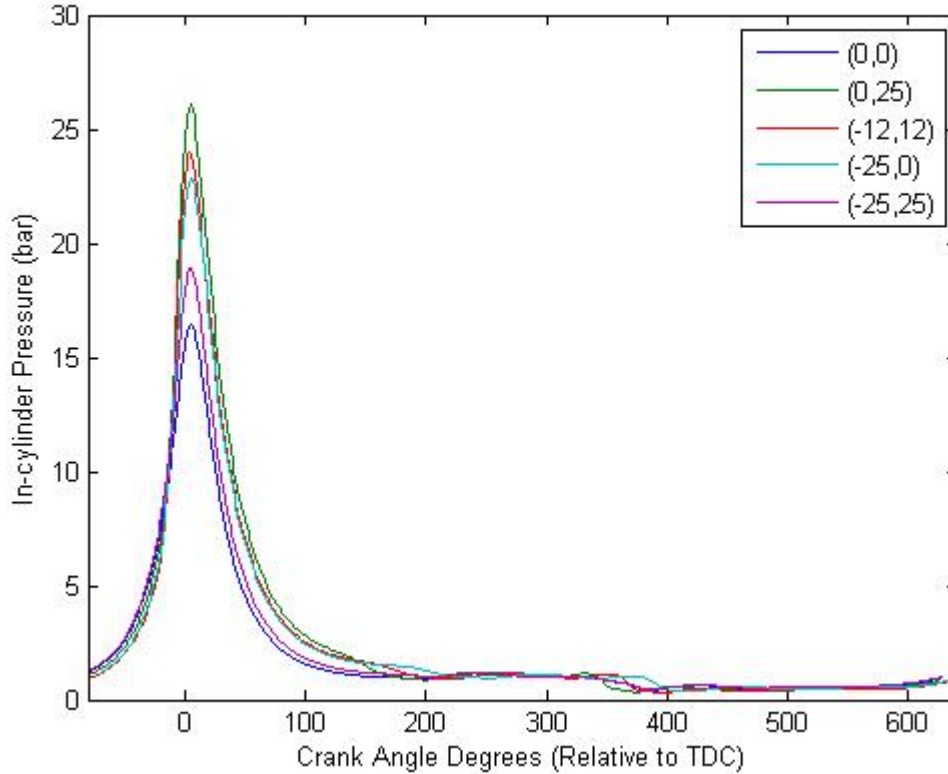


Figure 57: In-cylinder Pressure Evolution (2000 rpm, 0.49 bar)

The effect of cam timing can also be seen in the mass fraction burned curve as shown in Figure 58. The start of combustion varies about 4 degrees and the duration varies about 3 degrees. More important that these two parameters is the overall curvature of the graphs. The shapes are similar, but still show significant variation. The quickest burn occurs when both the cams are at 12 degrees. The slowest burn rate comes from a parked condition.

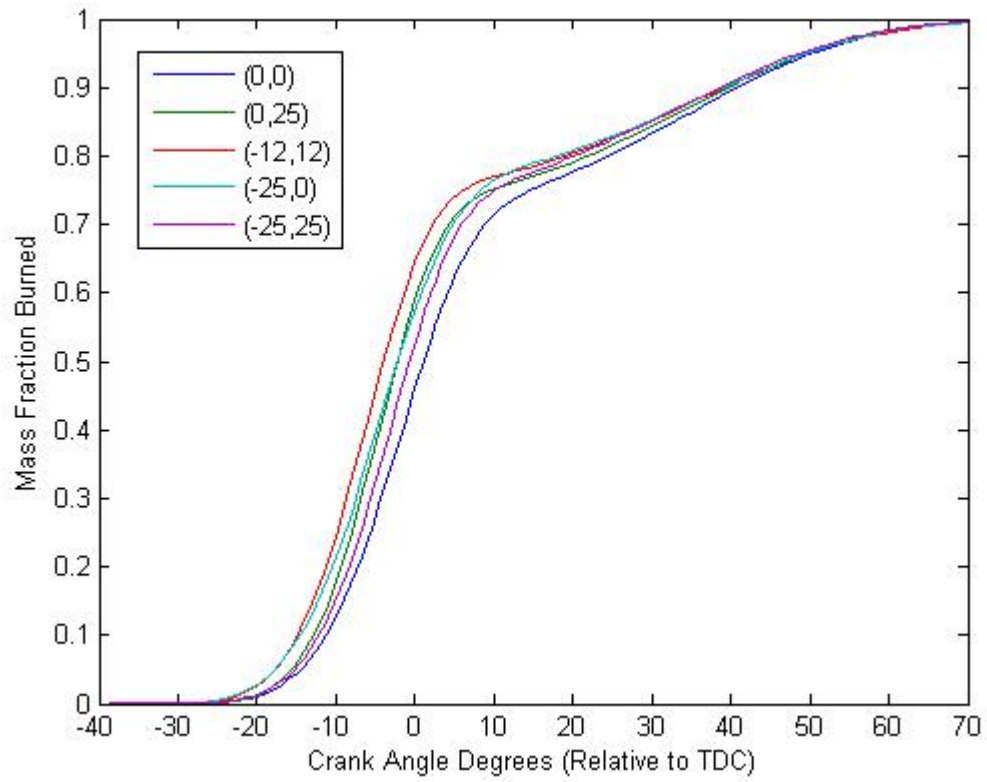


Figure 58: Variations in Mass Fraction Burned Curved (2000 rpm, 0.49 bar)

Chapter 6: Conclusions

Choosing a cam pair requires a compromise between several parameters. These parameters include the torque output (IMEP), the trapped air mass, the residual air mass, the volumetric efficiencies and fuel efficiency. The optimum cam position also depends on several external conditions. Depending on the target condition, each parameter's importance shifts. During heavy accelerations maximizing torque output is the main goal. During heavy deceleration fuel efficiency is the most important. Often times the fuel ratio is leaned to further reduce the fuel consumed. There are several other conditions where the optimum cam pairs must be a compromise of several parameters. All load conditions between hard acceleration and hard deceleration will have a different optimum cam pair. For some conditions reducing emissions is the most important. In these situations the trapped residual gases would be increased by increasing the valve overlap. Other conditions have fuel efficiency or torque output as the paramount factors. For most cases the cam pair with the highest volumetric efficiency that satisfies the residual requirement and meets the torque demand would be chosen.

In addition to normal running conditions, several special situations require still different cam pairs. Gear shifts, idle, cold start, engine warm-up and sensor malfunctions all have unique requirements and cam pairs. Therefore it is important to have a method of determining the effect cam phasing will have on each parameter. As shown in this thesis, an engine model can be created from a relatively small set of experimental data. If this model is then validated by another set of data, then the model can be used to accurately explore a broad range of engine conditions. Engine simulations based on an engine model take a considerably shorter amount of time compared to dynamometer test

cells. In addition an engine simulation can run in regions where an engine on a test cell cannot normally go. Overall, engine modeling is a cost effective way to rapidly optimize the controllable parameters of an internal combustion engine.

Chapter 7: Future Research

The experimental data used to generate the model was taken on an engine dynamometer. In industry a standard cycle of testing is usually performed. Once the physical design of an engine is performed, engine dynamometer testing is usually performed. At this stage in development, the final vehicle design is not complete and a prototype vehicle is not usually available. In addition an engine test cell is much smaller and easier to run than a chassis dynamometer or in-vehicle testing. Therefore, engine dynamometer testing is initially performed to gain preliminary data. Steady-state data is more easily dealt with than transient data. An engine dynamometer is proficient at maintaining constant conditions.

An engine on a dynamometer does not perfectly parallel an engine on a vehicle. Firstly, an engine on a vehicle has several accessory loads that are not present on an engine on a dynamometer. Secondly, all of the conditions in a test cell including temperature and pressure are closely. A vehicle encounters temperatures and precipitation that cannot be simulated in a test cell. The cooling system on vehicle also cannot be simulated in a test cell. An engine is cooled by air flow through a radiator and directly by air flow over the engine and powertrain system. Lastly the dynamics of a transmission system are not present. Because of these reasons, it is important to also test an engine on a vehicle. To ensure that the vehicle data agrees with the dynamometer and GT-Power data, in-vehicle data will be taken. The in-vehicle data is not expected match

perfectly. Parameters such as the intake and exhaust wall temperatures will be different from the dynamometer data, but temperature invariant outputs such as volumetric efficiency should be constant. Any discrepancies between the GT-Power model and the in-vehicle data will be analyzed and resolved.

References

- Centro Ricerche Fiat (CRF), European Powertrain Conference, 2002.
- Diana, S., Giglio, V., Iorio, B., and Police, G., “Evaluation of the Effect of EGR on Engine Knock”, SAE Paper 982479, 1998.
- FEV Motortechnik GmbH, European Powertrain Conference, 2002.
- Gamma Technologies. “GT-Power User’s Manual, Version 6.1.” 2004.
- Guezennec, Yann G., Internal Combustion Engine Fundamentals, Technical Presentation, 2003.
- Hatano, K., Iida, K., Higashi, H., and Murata, S., “Development of a New Multi-Mode Variable Valve Timing Engine”, SAE Paper 930878, 1993.
- Heywood, J. B., *Internal Combustion Engine Fundamentals*, McGraw-Hill, 1988.
- Kramer, Ulrich and Philips, Patrick, “Phasing Strategy for an Engine with Variable Cam Timing”, SAE Paper 2002-01-1101.
- Leone, T. G., Christenson, E. J., and Stein, R. A., “Comparison of Variable Camshaft Timing Strategies at Part Load”, SAE Paper 960584, 1996.
- Moriya, Y., Watanabe, A., Uda, H., Kawamura, H., Yoshioka, M., and Adachi, M., “A Newly Developed Intelligent Variable Valve Timing System – Continuously Controlled Cam Phasing as Applied to a New 3 Liter Inline 6 Engine”, SAE Paper 960579, 1996.
- Parvate-Patil, G. B. and Gordon B., “An Assessment of Intake and Exhaust Philosophies For Variable Valve Timing”, SAE Paper 2003-32-0078.
- Pierik, R. J. and Burkhard, J. F., “Design and Development of a Mechanical Variable Valve Actuation System”, SAE Paper 2000-01-1221, 2000.
- Sellnau, Mark and Rask, Eric, “Two-Step Variable Valve Actuation for Fuel Economy, Emissions, and Performance”, SAE Paper 2003-01-0029.
- Tabaczynski, R., Ford Technical Fellow, Ohio State mechanical engineering department seminar, 2/1/2002.